Inorganic Chemistry

Article

pubs.acs.org/IC

μ-η^6,η^6-Arene-Bridged Diuranium Hexakisketimide Complexes Isolable in Two States of Charge

Paula L. Diaconescu*[,†] and Christopher C. Cummins*[,‡]

[†]Department of Chemistry & Biochemistry, University of California, Los Angeles, California 90095, United States

[‡]Department of Chemistry, Massachusetts Institute of Technology, Cambridge, Massachusetts 02139, United States

Supporting Information

ABSTRACT: Diuranium μ-η^6,η^6-arene complexes supported by ketimide ligands were synthesized and characterized. Disodium or dipotassium salts of the formula $M_2(\mu\text{-}\eta^6,\eta^6\text{-arene})[U(NC^tBuMes)_3]_2$ (M = Na or K, Mes = 2,4,6-$C_6H_2Me_3$) and monopotassium salts of the formula $K(\mu\text{-}\eta^6,\eta^6\text{-arene})[U(NC^tBuMes)_3]_2$ (arene = naphthalene, biphenyl, *trans*-stilbene, or *p*-terphenyl) were both observed. Two different salts of the monoanionic, toluene-bridged complexes are also described. Density functional theory calculations have been employed to illuminate the electronic structure of the μ-η^6,η^6-arene diuranium complexes and to facilitate the comparison with related transition-metal systems, in particular $(\mu\text{-}\eta^6,\eta^6\text{-}C_6H_6)[VCp]_2$. It was found that the μ-η^6,η^6-arene diuranium complexes were isolobal with $(\mu\text{-}\eta^6,\eta^6\text{-}C_6H_6)[VCp]_2$ and that the principal arene-binding interaction was a pair of δ bonds (total of 4e) involving both metals and the arene lowest unoccupied molecular orbital. Reactivity studies have been carried out with the mono- and dianionic μ-η^6,η^6-arene diuranium complexes, revealing contrasting modes of redox chemistry as a function of the system's state of charge.

INTRODUCTION

Metal complexes involving the π system of benzene and related aromatic hydrocarbons have been of long-standing interest because of the fundamental nature of such species.[1] The situation is particularly interesting when the metal, as is the case for uranium, possesses both d and f valence orbitals capable of covalent interactions.[2] The first crystallographically characterized uranium benzene complex, $U(\eta^2\text{-}AlCl_4)_3(\eta^6\text{-}C_6H_6)$, was reported in 1971 by Cesari et al.,[3] who observed an average U−C distance of 2.91 ± 0.01 Å and an average C−C distance of 1.39 Å for the planar η^6-bound benzene ring. The latter distance compares well with the 1.397(1) Å distance for free benzene.[4,5] In 1987, Cotton and Schwotzer described the analogous hexamethylbenzene complex, reporting an average U−C distance of 2.93(2) Å;[6] other arene complexes were also reported.[7,8] A related finding was a uranium(III) homoleptic alkoxide complex obtained as a dimer by virtue of η^6-arene binding,[9] with the observed U−C distances essentially identical with those reported for Cesari's benzene complex. Furthermore, actinide bis(arene) sandwich complexes including $U(\eta^6\text{-}C_6H_6)_2$ have been studied by computational methods.[10,11]

In 2000, we reported a new structural motif for arene coordination to uranium, namely, the inverted sandwich formed between a bridging aromatic hydrocarbon and two uranium centers via μ-η^6,η^6 interactions.[12] The first such complexes were neutral species of the formula $(\mu\text{-}\eta^6,\eta^6\text{-arene})[U(N[R]Ar)_2]_2$ [R = ^{t}Bu or 1-adamantyl (Ad); arene = benzene or toluene; Ar = 3,5-$C_6H_3Me_2$].[12] The molecular structure of $(\mu\text{-}\eta^6,\eta^6\text{-toluene})[U(N[Ad]Ar)_2]_2$ revealed both substantially shorter U−C distances [average 2.594(9) Å] and longer C−C distances [average 1.438(13) Å] than those previously observed for any uranium complex of a benzene derivative. This large structural perturbation has been explained in terms of covalent 4e, δ back-bonding from the two U centers to the bridging arene ligand; the δ back-bonds have been visualized with the aid of density functional theory (DFT) calculations, which reproduce rather accurately the key structural parameters.[12] While the U−arene bonding renders the assignment of a formal oxidation state to the U centers in such systems problematic,[13] the complexes serve as synthons for divalent uranium.[14,15]

The inverted sandwich motif has been known both in transition-metal chemistry,[16−21] as exemplified by the triple-decker $(\mu\text{-}\eta^6,\eta^6\text{-}C_6H_6)[CpV]_2$ with an average C−C distance of 1.443(5) Å,[16] and in lanthanide chemistry, as exemplified by Lappert's anion $[(Cp^{tt}{}_2La)_2(\mu\text{-}\eta^6,\eta^6\text{-}C_6H_6)]^-$ (Cp^{tt} = η^5-1,3-^{t}Bu$_2$C$_5$H$_3$).[22,23] Lappert and co-workers formulated the latter system as an ionic aggregate containing two La^{II} ions and the benzene radical anion $C_6H_6^{\bullet-}$ on the basis of the observed benzene C−C distances that average 1.44(1) Å.[22,23] In related work involving anthracene as the bridging ligand, a μ-η^3,η^3-bonding mode was observed for $(Cp^*{}_2La)_2(\mu\text{-}C_{14}H_{10})$ rather than μ-η^6,η^6, similarly consistent with the ionic inclusion of a reduced aromatic hydrocarbon amidst lanthanide cations.[24] Before our work with uranium, covalent bonding was not invoked to explain sandwiching of a benzene derivative by any of the f elements.

The closest precedent for our arene-bridged diuranium compounds is that of Ephritikhine and co-workers, who reported a μ-η^7,η^7-cycloheptatrienyldiuranium sandwich complex, the anionic component of $[U(BH_4)_2(OC_4H_8)_5][(\mu\text{-}\eta^7,\eta^7\text{-}C_7H_7)[U(BH_4)_3]_2]$.[25,26] Although a detailed description of the electronic structure was not included, it was suggested that the μ-η^7,η^7-C_7H_7 ring should be described as an aromatic trianion and the metals as U^{IV} ions. We believe that this suggestion is consistent with the notion that the four electrons in the doubly

Received: October 5, 2011
Published: February 16, 2012

   dx.doi.org/10.1021/ic202163m | *Inorg. Chem.* 2012, 51, 2902−2916

degenerate $C_7H_7^{3-}$ highest occupied molecular orbital (HOMO; δ symmetry with respect to the U−U internuclear axis) engage in covalent δ bonding with the two U centers; such a description is equivalent to that advanced by us for the isolobal (μ-η^6,η^6-arene)[U(N[R]Ar)$_2$]$_2$ complexes.[12]

Although bridging benzene or toluene uranium complexes have been reported recently,[27−32] analogous uranium complexes of other aromatic hydrocarbons had not been forthcoming. In order to extend the class of μ-η^6,η^6-arene diuranium complexes, a new ancillary ligand, the ketimide NC^{t}BuMes (Mes = 2,4,6-$C_6H_2Me_3$) was investigated and led to the report of a reactive dianionic μ-η^6,η^6-naphthalene complex K_2(μ-η^6,η^6-$C_{10}H_8$)[U(NC^{t}BuMes)$_3$]$_2$ (K_2[μ-naph-**1**$_2$]).[33] This system uniquely incorporates a planar naphthalene ligand with both U atoms interacting in a symmetrical η^6 fashion to the *same* ring of the naphthalene bridge. This structural motif is different from that known for lanthanides, which coordinate to opposites sides of the two aromatic rings.[1,34−49] Herein we report that the ketimide ligand allows the synthesis of other μ-η^6,η^6-arene complexes as well; the new system contrasts with the amide system's neutral status by generating mono- and dianionic complexes. A synthetic protocol was developed that does not require the use of the arene as the solvent, allowing expansion of this class to biphenyl, *trans*-stilbene, and *p*-terphenyl derivatives. Finally, computational methods have been used to probe the electronic structure of these complexes; in addition, they allowed us to recognize the isolobal relationship between diuranium inverted sandwiches and prototypical triple-decker transition-metal sandwich complexes.

RESULTS AND DISCUSSION

Synthesis and Characterization of Dianionic μ-η^6,η^6-Arene Diuranium Complexes. As was reported previously, the iodide trisketimide uranium(IV) starting material UI(NC^{t}BuMes)$_3$(DME) (**1**-I(DME), DME = 1,2-dimethoxyethane)[33] reacts smoothly with 4 equiv of KC_8 and 0.5 equiv of naphthalene in DME, leading to the naphthalene-bridged complex K_2[μ-naph-**1**$_2$] in 60% yield as a dark-brown powder.[33] The μ-η^6,η^6 formulation for the $C_{10}H_8$ bridge was established by X-ray crystallography.[33] The dianion of K_2[μ-naph-**1**$_2$] is related to the neutral systems (μ-η^6,η^6-arene)[U(N[R]Ar)$_2$]$_2$ because it is comprised *formally* of two f^4 [U(NC^{t}BuMes)$_3$]$^-$ fragments conjoined by a neutral arene bridge. The structure of K_2[μ-naph-**1**$_2$] is unusual because known d-block dimetal complexes with a bridging naphthalene ligand prefer coordination of the two metal centers to opposite ends of the aromatic bridge. Systems of the latter type are referred to as "slipped triple-decker" complexes.[50,51]

A key result of the present work is the extension of the synthetic strategy used to prepare K_2[μ-naph-**1**$_2$] to other aromatic hydrocarbons (Chart 1). Thus, the treatment of **1**-I(DME) with 4 equiv of KC_8 in the presence of stoichiometric amounts of the desired arene is a general synthetic route for obtaining dipotassium salts of the dianions [(μ-η^6,η^6-arene)[U(NC^{t}BuMes)$_3$]$_2$]$^{2-}$ (arene = biphenyl, K_2[μ-biph-**1**$_2$]; *trans*-stilbene, K_2[μ-stilb-**1**$_2$]; *p*-terphenyl, K_2[μ-terph-**1**$_2$]). The pentane solubility of these systems qualitatively increases in the following order: naphthalene < biphenyl < *trans*-stilbene ≈ *p*-terphenyl (i.e., K_2[μ-naph-**1**$_2$] is slightly soluble in *n*-pentane, while K_2[μ-terph-**1**$_2$] dissolves readily in it). The corresponding disodium salts could also be obtained by using sodium as the reductant, indicating that K ion incorporation is not required to stabilize the dianionic inverted sandwiches. The disodium salts have proven to be highly lipophilic, hampering their recrystallization from *n*-pentane and leading to relatively low isolated yields.

Chart 1. Dianions Prepared as Disodium or Dipotassium Salts by Reduction of 1-I(DME) in the Presence of Stoichiometric Amounts of Arene[a]

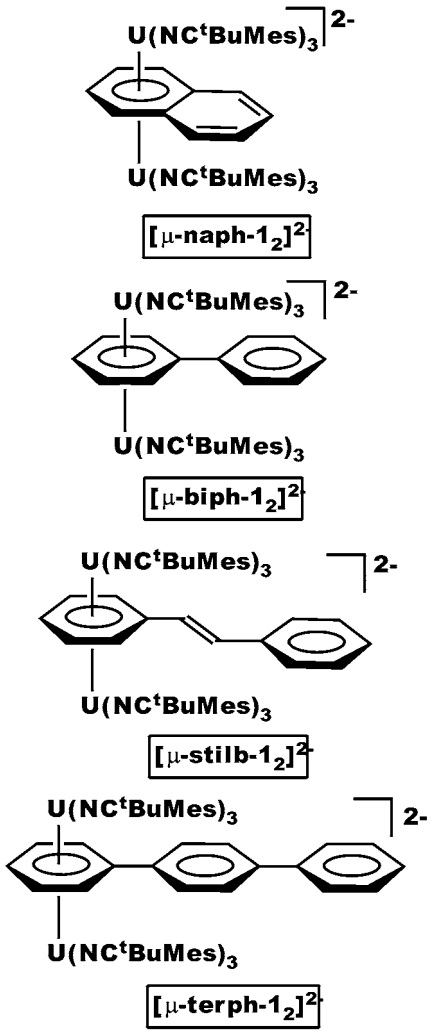

[a]Isolated yields of crystalline substances: K_2[μ-naph-**1**$_2$], 60%; K_2[μ-biph-**1**$_2$], 56%; Na_2[μ-naph-**1**$_2$], 57%; K_2[μ-stilb-**1**$_2$], 63%; K_2[μ-terph-**1**$_2$], 67%.

Compounds [Na_2(OEt_2)][μ-biph-**1**$_2$] and K_2[μ-stilb-**1**$_2$] were structurally characterized by single-crystal X-ray diffraction (Figures 1 and 2). This study allows the comparison of C−C distances in a sandwiched versus a pendant phenyl ring. Table 1 shows distances of ca. 1.44 Å for the complexed ring[12] and values close to that of unperturbed benzene [1.397(1) Å] for the pendant ring.[4,5] In the case of [Na_2(OEt_2)][μ-biph-**1**$_2$], the tight and symmetrical μ-η^6,η^6-biphenyl complexation is revealed clearly by the short interatomic distances [average 2.627(8) Å] between U1/U2 and C71−C76. Furthermore, the C−C distances in the sandwiched ring are similar [average 1.442(10) Å] and longer than those in the pendant biphenyl ring [average 1.387(16) Å]. Crystalline biphenyl is planar (D_{2h}) at 110 K, with aromatic C−C distances varying between 1.379(3) and 1.399(3) Å [average 1.390(3) Å].[52−54] On the

dx.doi.org/10.1021/ic202163m | Inorg. Chem. 2012, 51, 2902−2916

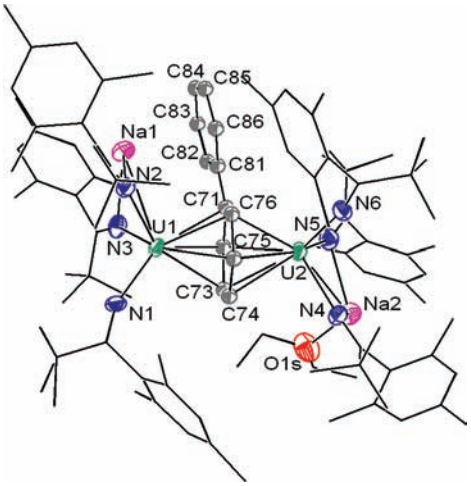

Figure 1. Structural drawing of $[Na_2(OEt_2)][\mu\text{-biph-}\mathbf{1}_2]$ with thermal ellipsoids at the 50% probability level; all H atoms have been omitted for clarity. See Table 1 for selected interatomic distances.

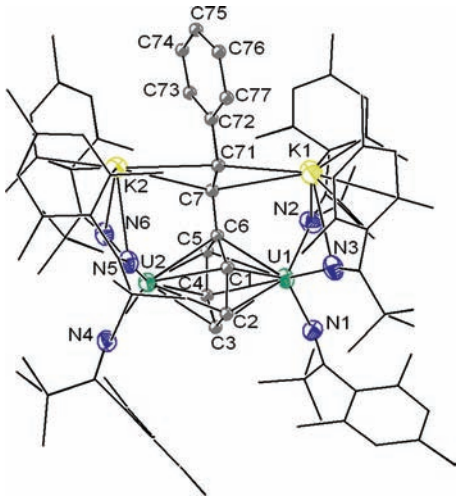

Figure 2. Structural drawing of complex $K_2[\mu\text{-stilb-}\mathbf{1}_2]$ with thermal ellipsoids at the 50% probability level; H atoms have been omitted for clarity. See Table 1 for selected interatomic distances.

other hand, biphenyl adopts a twisted structure (D_2) in solution, with a central torsion angle of 32 ± 2°; the two phenyl rings are only weakly conjugated favoring the planar structure, while ortho H···H repulsions induce a twist.[55] The biphenyl ligand of $[Na_2(OEt_2)][\mu\text{-biph-}\mathbf{1}_2]$ displays a minimal distortion from planarity, as indicated by the values of the two torsion angles C72−C71−C81−C82 and C76−C71−C81−C86 (−1.5 and 3.2°, respectively). The C71−C81 distance between the two phenyl rings is 1.455(10) Å, as compared to 1.496(3) Å for free biphenyl.[54] The contraction of the inter-ring junction is known for various biphenyl excited states as well as for the biphenyl radical anion.[55] In summary, the major structural change experienced by biphenyl upon the formation of $[Na_2(OEt_2)][\mu\text{-biph-}\mathbf{1}_2]$ is expansion of the C−C distances by 0.05 Å specifically in the ring undergoing η^6,η^6 complexation.

Other $[Na_2(OEt_2)][\mu\text{-biph-}\mathbf{1}_2]$ structural parameters of interest include the U−N distances, of which two are long and one is short for each U atom: the U1−N2 and U1−N3 distances are ca. 0.1 Å longer than U1−N1, likely because N2 and N3 are involved in a side-on interaction with the Na cation.

Table 1. Selected Interatomic Distances and Angles for Structures of New $\mu\text{-}\eta^6,\eta^6$-Arene Diuranium Complexes

	$[Na_2(OEt_2)]$ $[\mu\text{-biph-}\mathbf{1}_2]$	K_2 $[\mu\text{-stilb-}\mathbf{1}_2]$	$[K_2I]$ $[\mu\text{-tol-}\mathbf{1}_2]$	$[K(DME)]$ $[\mu\text{-tol-}\mathbf{1}_2]$
C−C avg. for $\mu\text{-}\eta^6,\eta^{6n}$ arene	1.442(10)	1.439(14)	1.45(2)	1.405(15)
C−C avg. for pendant C_6H_5	1.387(14)	1.365(22)		
U1−C avg.	2.621(7)	2.670(9)	2.663(13)	2.594(10)
U2−C avg.	2.633(7)	2.646(9)	2.632(13)	2.641(10)
U1−N avg., terminal	2.240(6)	2.208(7)	2.209(10)	2.239(7)
U1−N avg., μ-Na or K	2.331(6)	2.256(8)	2.237(12)	2.245(8)
U2−N avg., terminal	2.233(6)	2.222(8)	2.215(10)	2.209(8)
U2−N avg., μ-Na or K	2.319(6)	2.274(8)	2.236(12)	
NUN avg.	96.4(2)	98.5(3)	99.1(4)	99.5(3)
UNC avg., terminal	162.1(5)	164.8(7)	171.1(10)	174.3(8)
UNC avg., μ-Na or K	157.4(6)	169.0(8)	171.0(12)	164.1(8)

The same situation is found for N4 and N5, which, being proximal to Na2, exhibit distances to U2 longer by ca. 0.1 Å than the U2−N6 distance. Both Na1 and Na2 can be viewed as approximately five-coordinate. In the case of Na1, in addition to N2 and N3, there are close contacts to aryl rings. In the case of Na2, the fifth interaction is to the diethyl ether O1s. The interaction between Na1 and C81 (pendant phenyl *ipso*-C) accounts for the gentle curvature of the complexed biphenyl ligand. The electrostatic solvation of alkali-metal cations by aromatic residues is a well-documented phenomenon.[56−59]

The structural picture of $K_2[\mu\text{-stilb-}\mathbf{1}_2]$ (Figure 2 and Table 1) is similar to that of $[Na_2(OEt_2)][\mu\text{-biph-}\mathbf{1}_2]$, presenting the following key features: (1) elongation of C−C distances in the complexed ring relative to the pendant phenyl; (2) inclusion of roughly five-coordinate K cations, which each interact with two ketimide N atoms, two mesityl rings, and the stilbene double bond; (3) U centers experiencing a three-legged piano-stool coordination environment.

Synthesis and Characterization of Monoanionic $\mu\text{-}\eta^6,\eta^6$-Arene Diuranium Complexes. The optimum synthesis of the dianions described above was found through trial and error to consist of treatment of the soluble, molecular uranium(IV) starting material **1**-I(DME) with an excess of potassium graphite (KC_8, 4 equiv per U) along with a stoichiometric amount of the arene to be complexed, in DME solvent (Chart 1). Because of the production of the diuranium inverted sandwiches from **1**-I(DME) requires two electrons per U center, 2 equiv of KC_8 per U was used in an effort to optimize the procedure. Those conditions resulted in the formation of new, isolable, inverted sandwiches having only a single negative charge, namely, the series of $K(\mu\text{-}\eta^6,\eta^6\text{-arene})[U(NC^tBuMes)_3]_2$ ($K[\mu\text{-arene-}\mathbf{1}_2]$, Chart 2). The formation of these complexes starting from **1**-I(DME) is a process requiring three electrons total; as such, $K[\mu\text{-arene-}\mathbf{1}_2]$ represent intriguing examples of mixed-valent diuranium systems with short interuranium distances (see below). Mixed-valent diuranium complexes are not common,[60−63] and the question of possible valence delocalization in such systems represents a problem of considerable fundamental interest. Burns and co-workers discussed this subject with reference to a $U^{V/VI}_2$ system having a crystallographic center of symmetry relating the two U nuclei and bridging imido ligands potentially capable of mediating electronic delocalization.[60]

dx.doi.org/10.1021/ic202163m | *Inorg. Chem.* 2012, 51, 2902−2916

Chart 2. Monoanions [μ-arene-$\mathbf{1}_2$]$^-$ Prepared as Potassium Salts by Reduction of 1-I(DME) with 2 equiv of KC_8 in the Presence of Arene[a]

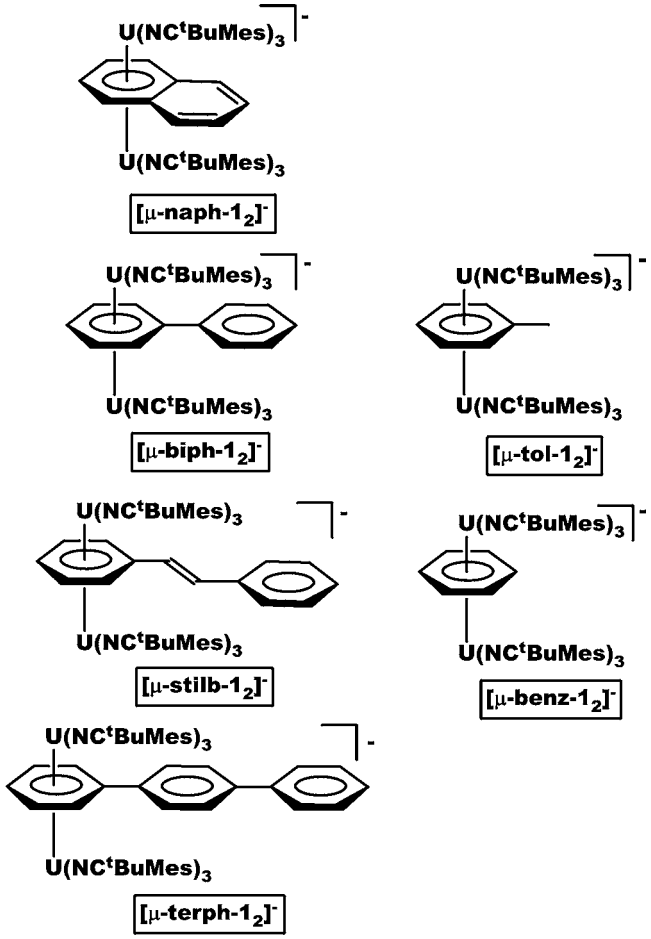

[a]Isolated yields of crystalline substances: K[μ-naph-$\mathbf{1}_2$], 56%; K[μ-biph-$\mathbf{1}_2$], 42%; K[μ-stilb-$\mathbf{1}_2$], 83%; K[μ-terph-$\mathbf{1}_2$], 69%; [K(DME)][μ-tol-$\mathbf{1}_2$], 41%; [K_2I][μ-tol-$\mathbf{1}_2$], 44%; [K(DME)][μ-benz-$\mathbf{1}_2$], 11%.

Interestingly, while unavailable in the series of K_2[μ-arene-$\mathbf{1}_2$], inverted sandwiches with the bridging ring as benzene or toluene could be obtained in the series of K[μ-arene-$\mathbf{1}_2$] (Chart 2). We speculate that highly conjugated arenes such as *trans*-stilbene or naphthalene support the extra charge in K_2[μ-arene-$\mathbf{1}_2$] by virtue of delocalization; this point merits further study by computational means. In addition, toluene is generally less oxidizing than the other arenes employed;[64] stated alternatively, toluene is the least δ-acidic of the arenes studied herein.

The toluene complexes were isolated with two different formulations: [K(DME)][μ-tol-$\mathbf{1}_2$] and [K_2I][μ-tol-$\mathbf{1}_2$], both crystallographically characterized (Figures 3 and 4). In both structures (Table 1), the toluene ligand bridges the two U atoms in a μ-η^6,η^6 fashion, with all U−C distances close to 2.6 Å, as was the case for K_2[μ-arene-$\mathbf{1}_2$]. While the included K_2I cation provides a coordination environment identical for both U atoms, the included K(DME) cation places the K ion close to only one of the two U centers (U1 in Figure 3). Structural parameters support this dichotomy: in [K(DME)][μ-tol-$\mathbf{1}_2$], the terminal U1−N (side that complexes K) distances are longer by ca. 0.03 Å than the terminal U2−N distances. In addition, the U1−C bonds are shorter than the U2−C bonds

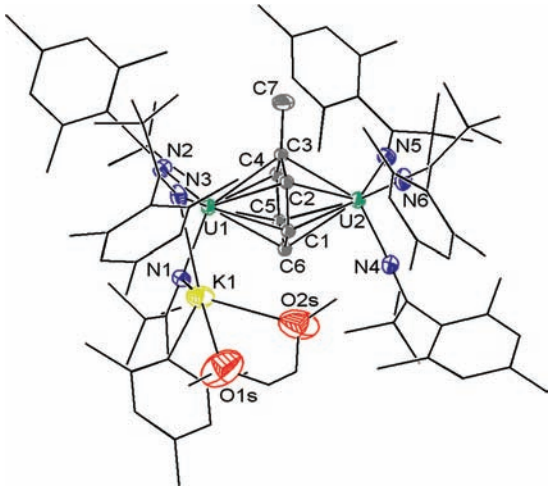

Figure 3. Structural drawing of complex [K(DME)][μ-tol-$\mathbf{1}_2$] with thermal ellipsoids at the 50% probability level. Only one of the two crystallographically distinct but chemically equivalent molecules is shown; H atoms have been omitted for clarity. See Table 1 for selected interatomic distances.

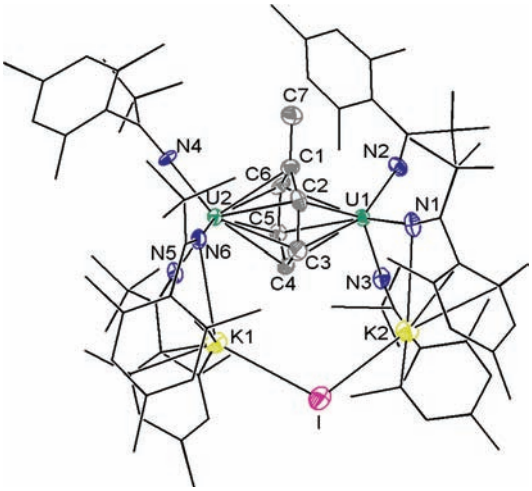

Figure 4. Structural drawing of complex [K_2I][μ-tol-$\mathbf{1}_2$] with thermal ellipsoids at the 50% probability level; H atoms have been omitted for clarity. See Table 1 for selected interatomic distances.

by 0.05 Å. In the case of [K_2I][μ-tol-$\mathbf{1}_2$], C and N distances to both U centers are essentially the same. Comparison of the two structures leads to the notion that both the nature of the cation and the mode of its inclusion may significantly influence the degree of charge delocalization.

NMR Spectroscopic Characterization of Inverted Sandwich Uranium Complexes. The chemical shifts for the protons/deuterons of the bridging ring of μ-η^6,η^6-arene diuranium complexes are diagnostic. For the parent system (μ-η^6,η^6-C_6H_6)[U(N[R]Ar)$_2$]$_2$, the single signal for the bridging benzene ligand was found at ca. −80 ppm by ^{1}H or ^{2}H NMR spectroscopy.[12] For (μ-η^6,η^6-toluene)[U(N[R]Ar)$_2$]$_2$, the bridging toluene methyl resonance was found near +20 ppm, while the ring protons were characterized by three resonances in the −60 to −80 ppm range.[12] These data generate an expectation that the μ-η^6,η^6 rings associate with strong upfield chemical shifts for protons or deuterons directly attached to the bridging ring.

dx.doi.org/10.1021/ic202163m | *Inorg. Chem.* 2012, 51, 2902−2916

As was reported previously,[33] disodium or dipotassium salts of $[\mu\text{-naph-}\mathbf{1}_2]^{2-}$ evince four signals for the bridging naphthalene ligand, showing that the U centers do not move back and forth between the two fused six-membered rings on the ^{1}H and ^{2}H NMR spectroscopy time scales. The same is also true for the naphthalene-bridged monoanion $[\mu\text{-naph-}\mathbf{1}_2]^-$. Of further importance for $[\mu\text{-naph-}\mathbf{1}_2]^{2-}$ is the observation of a single ketimide ligand environment, implying mobility of the associated alkali-metal ions. The situation is less clear for $[\mu\text{-naph-}\mathbf{1}_2]^-$, in that more ^{1}H NMR resonances are found than the four expected for a single ketimide ligand environment; unambiguous assignment of the ancillary ketimide ligand resonances for monoanions $[\mu\text{-arene-}\mathbf{1}_2]^-$ is generally complicated by the presence of broad and overlapping signals. Chemical shift assignments for the bridging naphthalene in both $[\mu\text{-naph-}\mathbf{1}_2]^{2-}$ and $[\mu\text{-naph-}\mathbf{1}_2]^-$ were facilitated by deuterium labeling and ^{2}H NMR studies (Chart 3).

Chart 3. Salts $K_2[\mu\text{-naph-}\mathbf{1}_2]\text{-}d_n$ and $K[\mu\text{-naph-}\mathbf{1}_2]\text{-}d_n$ Prepared from the Corresponding Naphthalene Isotopomers To Facilitate Chemical Shift Assignments[a]

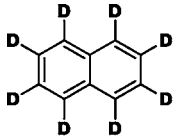

$K_2[\mu\text{-naph-}\mathbf{1}_2]$: +112,* -32, -43, -142*
$K[\mu\text{-naph-}\mathbf{1}_2]$: -0.5, -39, -118,* -126*

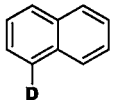

$K_2[\mu\text{-naph-}\mathbf{1}_2]$: -43, -142*
$K[\mu\text{-naph-}\mathbf{1}_2]$: -0.4, -117*

[a]Observed ^{2}H NMR signals (ppm) are as indicated (20 °C). Signals marked with an asterisk were relatively broad and were assigned to the six-membered ring undergoing $\mu\text{-}\eta^6,\eta^6$ complexation.

Isotopomers of the biphenyl-bridged anions $K_2[\mu\text{-biph-}\mathbf{1}_2]$ and $K[\mu\text{-biph-}\mathbf{1}_2]$ were also prepared for NMR spectroscopic investigation, as indicated in Chart 4. The observation in both

Chart 4. $K_2[\mu\text{-biph-}\mathbf{1}_2]\text{-}d_n$ and $K[\mu\text{-biph-}\mathbf{1}_2]\text{-}d_n$ Prepared from the Corresponding Biphenyl Isotopomers To Facilitate Chemical Shift Assignments[a]

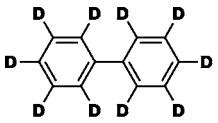

$K_2[\mu\text{-biph-}\mathbf{1}_2]$: 34,* -6, -21, -47, -80,* -126*
$K[\mu\text{-biph-}\mathbf{1}_2]$: 17, -9, -14, -84,* -141,* -165*

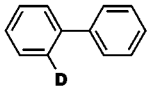

$K_2[\mu\text{-biph-}\mathbf{1}_2]$: -21, -125*
$K[\mu\text{-biph-}\mathbf{1}_2]$: -9, -165*

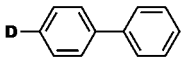

$K_2[\mu\text{-biph-}\mathbf{1}_2]$: 34,* -6
$K[\mu\text{-biph-}\mathbf{1}_2]$: -14, -83*

[a]Observed ^{2}H NMR signals (ppm) are as indicated (20 °C). Signals marked with an asterisk were relatively broad and were assigned to the phenyl ring undergoing $\mu\text{-}\eta^6,\eta^6$ complexation.

cases of six ^{2}H NMR signals associated with the bridging biphenyl for the anions prepared from biphenyl-d_{10} reveals C_{2v} symmetry, with the C_2 axis being coincident with the biphenyl ring junction. This means that the two U centers are statically affixed to just one of the two phenyl rings of the bridging biphenyl in solution at room temperature, consistent with the solid-state structures discussed above. Only a single ancillary ketimide ligand environment, identified by four peaks in the ^{1}H NMR spectrum of $K_2[\mu\text{-biph-}\mathbf{1}_2]$, is observed. Analogous to $K[\mu\text{-naph-}\mathbf{1}_2]$, the ^{1}H NMR spectrum of $K[\mu\text{-biph-}\mathbf{1}_2]$ is more complicated than that observed for the corresponding dianion.

In the case of the bridging *p*-terphenyl systems $K_2[\mu\text{-terph-}\mathbf{1}_2]$ and $K[\mu\text{-terph-}\mathbf{1}_2]$, the central phenylene ring or the terminal phenyl residues are, in principle, subject to diuranium complexation. Investigation of the ^{2}H NMR spectrum (77 MHz, Et_2O, 22 °C) of $K_2[\mu\text{-terph-}\mathbf{1}_2]\text{-}d_{14}$, prepared from *p*-terphenyl-d_{14}, revealed eight peaks at +22, +8, +6, +4, +3, −18, −50, and −124 ppm. The observation of eight peaks is consistent with terminal and static $\mu\text{-}\eta^6,\eta^6$ complexation of a phenyl residue, as pictured in Charts 1 and 2. If complexation were to take place at the central phenylene portion of *p*-terphenyl, then only four peaks would be observed. Similarly, the ^{2}H NMR spectrum (77 MHz, Et_2O, 22 °C) of $K[\mu\text{-terph-}\mathbf{1}_2]\text{-}d_{14}$ prepared from perdeuterio-*p*-terphenyl displayed exactly eight peaks at +19, +12, +8, +7, −6, −88, −146, and −162 ppm. These results are consistent with a structure in which the U centers are bound to the terminal ring for both $K_2[\mu\text{-terph-}\mathbf{1}_2]$ and $K[\mu\text{-terph-}\mathbf{1}_2]$. In the case of $K_2[\mu\text{-terph-}\mathbf{1}_2]$, a single ketimide ligand environment (four signals) is observed by ^{1}H NMR spectroscopy, consistent with alkali-metal cation mobility on the NMR time scale; the ^{1}H NMR spectrum of $K[\mu\text{-terph-}\mathbf{1}_2]$ is not well resolved.

Interestingly, although the monoanionic $[\mu\text{-arene-}\mathbf{1}_2]^-$ salts displayed complicated and not well resolved ^{1}H NMR spectra, the salts $[K_2I][\mu\text{-tol-}\mathbf{1}_2]$ and $[K(DME)][\mu\text{-tol-}\mathbf{1}_2]$ display simpler ^{1}H NMR spectra, with the expected number of signals (four) for a single ketimide ligand environment in solution at room temperature. To aid in assignment of the ^{1}H NMR spectrum of $[K_2I][\mu\text{-tol-}\mathbf{1}_2]$, the salt $[K_2I][\mu\text{-benz-}\mathbf{1}_2]$, with a $\mu\text{-}\eta^6,\eta^6$-benzene ligand, was synthesized and its ^{1}H NMR spectrum (500 MHz, C_6D_6, 22 °C) recorded. On the basis of the chemical shift of −45 ppm for the bridging benzene protons in $[K_2I][\mu\text{-benz-}\mathbf{1}_2]$, along with the relative intensities of peaks (500 MHz, toluene-d_8, 20 °C), the chemical shifts at +35, −38, −43, and −45 ppm were assigned, respectively, to the protons of the $\mu\text{-}\eta^6,\eta^6$-toluene ligand in $[K_2I][\mu\text{-tol-}\mathbf{1}_2]$ as follows: Ph*CH*$_3$, *o*- or *m*-*Ph*CH$_3$, *p*-*Ph*CH$_3$, and *o*- or *m*-*Ph*CH$_3$. The ^{1}H NMR spectra of $[K_2I][\mu\text{-tol-}\mathbf{1}_2]$ and $[K(DME)][\mu\text{-tol-}\mathbf{1}_2]$ show largely different chemical shifts for the bridging toluene ligand ($[K(DME)][\mu\text{-tol-}\mathbf{1}_2]$: 65, C*H*$_3$-toluene; −109, *o*- or *m*-toluene; −113, *o*- or *m*-toluene; −126, *p*-toluene). Although the characterization of the corresponding benzene complexes is in agreement with these chemical shifts, an explanation for this difference is not apparent.

Redox Interconversion between Mono- and Dianionic Inverted Sandwiches. As shown in Scheme 1, it was possible to effect the chemical one-electron oxidation of dianions $[\mu\text{-arene-}\mathbf{1}_2]^{2-}$ to the corresponding monoanions $[\mu\text{-arene-}\mathbf{1}_2]^-$. The oxidants $[Cp_2Fe][O_3SCF_3]$ and P_4 were found competent to carry out the indicated reactions on a preparative scale, with isolated yields of $K[\mu\text{-naph-}\mathbf{1}_2]$ being ca. 70%. The original intent for the P_4 reaction was to produce a uranium phosphide complex; presumably, P_4 was instead converted to a reduced form such as $(K_2P_4)_n$.[65] The chemical *reduction* of $[\mu\text{-naph-}\mathbf{1}_2]^-$ could be used preparatively to provide $[\mu\text{-naph-}\mathbf{1}_2]^{2-}$ in yields averaging 80%; potassium anthracenide was employed as the

dx.doi.org/10.1021/ic202163m | Inorg. Chem. 2012, 51, 2902−2916

Scheme 1. Chemical Interconversion between Mono- and Dianionic Diuranium Inverted Sandwiches[a]

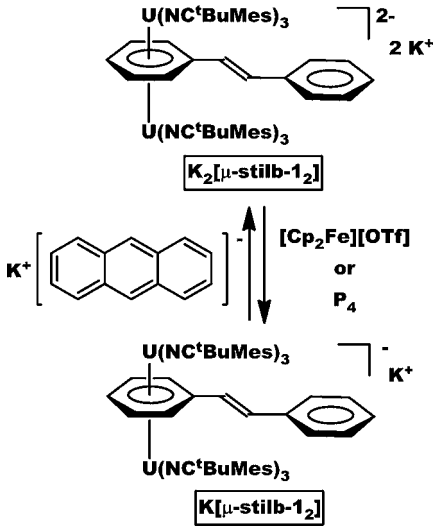

[a]In the example shown above, K[μ-stilb-$\mathbf{1}_2$] was reduced to K_2[μ-stilb-$\mathbf{1}_2$] with potassium anthracenide in 78% isolated yield. Alternatively, K_2[μ-stilb-$\mathbf{1}_2$] was oxidized to K[μ-stilb-$\mathbf{1}_2$] with either ferrocenium triflate in 81% isolated yield or white phosphorus in 69% yield. Interconversions involving the other K_2[μ-arene-$\mathbf{1}_2$]/K[μ-arene-$\mathbf{1}_2$] redox pairs proceeded similarly.

reductant. Notably, in the reduction reactions, no anthracene incorporation was observed. The reactions illustrated in Scheme 1 show that the chemical interconversion between the two states of the diuranium μ-η^6,η^6-arene inverted sandwich complexes can be executed successfully.

Other Reactions of Arene-Bridged Diuranium Hexakisketimide Anions. As was reported previously, the treatment of M_2[μ-naph-$\mathbf{1}_2$] (M = Na or K) with 2 equiv of 1,3,5,7-cyclooctatetraene afforded a mixture of two products: M[(COT)U(NC^{t}BuMes)$_3$] (M[**2**], **2** = [(COT)U(NC^{t}BuMes)$_3$]) and (μ-η^8,η^8-COT)U_2(NC^{t}BuMes)$_6$ (μ-COT-$\mathbf{1}_2$).[33] The latter compound is remarkable in possessing a COT ligand sandwiched between two trisketimidouranium fragments.[66] The reactions of all dipotassium salts K_2[μ-arene-$\mathbf{1}_2$] with 1,3,5,7-cyclooctatetraene provided K[**2**]. As was mentioned previously, Na_2[μ-naph-$\mathbf{1}_2$] forms Na[**2**] and μ-COT-$\mathbf{1}_2$ in a 1:1 ratio.[33] At the other extreme, Na_2[μ-biph-$\mathbf{1}_2$] forms only μ-COT-$\mathbf{1}_2$. It is important to note that while all of the COT reactions discussed take place within 2 h, the latter example requires 20 h for completion. Monitoring a diethyl ether solution of pure K[**2**] at room temperature, no formation of μ-COT-$\mathbf{1}_2$ was observed even after 23 h. In the case of the odd-electron species, a mixture of K[**2**] and μ-COT-$\mathbf{1}_2$ was always formed in different ratios. Therefore, K[**2**] can be synthesized from any even-electron species, Na[**2**] from Na_2[μ-naph-$\mathbf{1}_2$], and μ-COT-$\mathbf{1}_2$ from the reaction of **1**-I(DME) with M[**2**] (M = Na or K).[33]

Compounds M[**2**] can be oxidized to **2** (Figure 5) by reaction with $TiCl_4(THF)_2$ (used initially to test the formation of heterobimetallic COT complexes). As expected for a formally uranium(V) compound, the average U−C distance is shorter [2.715(30) Å] than that in μ-COT-$\mathbf{1}_2$ [2.822(15) Å]. Similar U^VCOT complexes have been reported; for example, (COT)U(NR$_2$)$_3$ (R = Me or Et) was also obtained by oxidation of the corresponding anion.[67,68]

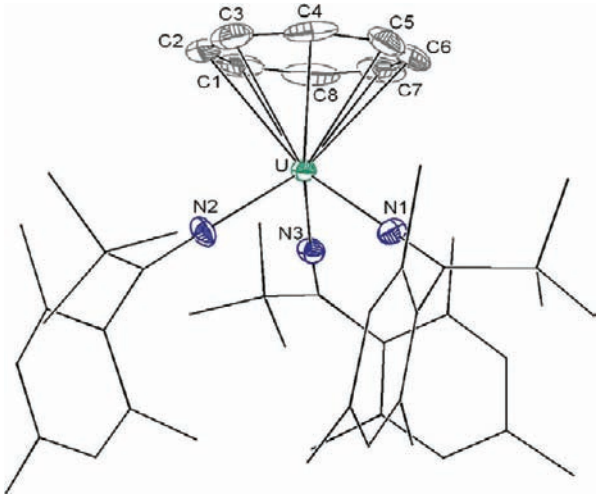

Figure 5. Structural drawing of complex **2** with thermal ellipsoids at the 50% probability level; H atoms were omitted for clarity. Selected distances (Å): U−N (avg.), 2.171(13); U−C (avg.), 2.715(30); C−C (avg.), 1.38(6).

In addition to the reactions with 1,3,5,7-cyclooctatetraene, it was found that Na_2[μ-naph-$\mathbf{1}_2$] reacted with diphenyl disulfide (2 equiv) to form a dark-yellow product, which was isolated in 60% yield (Scheme 2). The product was determined to be a dinuclear trithiolate-bridged uranium(IV) derivative, Na[(μ-SPh)$_3$$U_2$(NC^{t}BuMes)$_6$] (Na[**3**], **3** = [($\mu$-SPh)$_3$$U_2$(NC^{t}BuMes)$_6$]) by X-ray crystallography (Figure 6). Although the redox reaction involved the transfer of four electrons, as expected, it was found that the structure of the product is organized such that one Na ion is retained.

Rather surprising is the fact that the odd-electron, arene-bridged species K_2[μ-arene-$\mathbf{1}_2$] form K[**3**] in similar reactions. In the case of K[μ-arene-$\mathbf{1}_2$] reactions, 1.5 instead of 2 equiv of PhSSPh is used and these reactions involve the transfer of three electrons. It is probable that, in the reactions of M_2[μ-arene-$\mathbf{1}_2$] (M = Na or K), the other alkali-metal cation is eliminated as MSPh, although the identity of the byproducts was not established.

The reaction with azobenzene proceeded cleanly to a single major product in the case of the bridging toluene compounds [K(DME)][μ-tol-$\mathbf{1}_2$] and [K_2I][μ-tol-$\mathbf{1}_2$]. Even so, the reaction is not straightforward because the isolated product is the diuranium(V) complex (μ-NPh)$_2$$U_2$(NC^{t}BuMes)$_6$ (**4**; Figure 7), and five electrons are transferred during this reaction. K[PhNNPh], a known compound,[69] is proposed to be the byproduct, although its identity was not confirmed. This proposal is in accordance with the fact that the reaction with 2 equiv of PhNNPh is cleaner than the reaction with only 1 equiv of azobenzene.

Other K[μ-arene-$\mathbf{1}_2$] compounds also give **4** as a major product upon azobenzene treatment, but the reactions are not as clean as those of the toluene-bridged complexes. The reactions of K_2[μ-arene-$\mathbf{1}_2$] with PhNNPh have also been surveyed, but they are not as straightforward as those for [K(DME)][μ-tol-$\mathbf{1}_2$] and [K_2I][μ-tol-$\mathbf{1}_2$], even when the stoichiometry was adjusted to 3 equiv of PhNNPh.

General Bonding Considerations for μ-η^6,η^6-Arene-Bridged Diuranium Complexes. The bonding model proposed by us for the neutral amide model complexes (μ-η^6,η^6-C_6H_6)[U(NH$_2$)$_2$]$_2$ (Figure 8) considers them to be

dx.doi.org/10.1021/ic202163m | Inorg. Chem. 2012, 51, 2902−2916

Scheme 2. Preparation of M[3] (M = Na or K) from Either $M_2[\mu\text{-naph-}1_2]$ or $K[\mu\text{-naph-}1_2]$, with Loss of Naphthalene

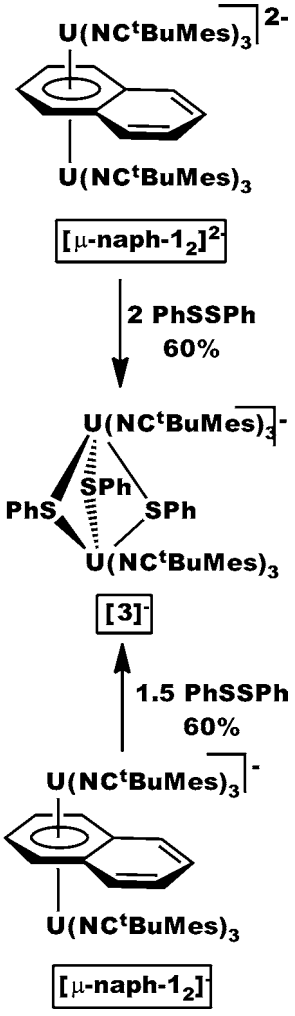

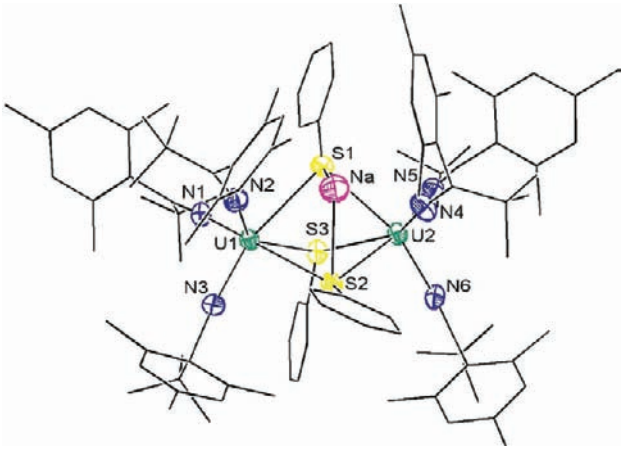

Figure 6. Structural drawing of complex Na[3] with thermal ellipsoids at the 50% probability level; H atoms were omitted for clarity.

S = 2 systems, with the four unpaired electrons occupying uranium-based orbitals. These orbitals are followed by one pair of degenerate δ bonds formed by the overlap of benzene's lowest unoccupied molecular orbital (LUMO; π^*, of δ symmetry with respect to the axis of interaction with uranium) and 5f orbitals of appropriate symmetry (of δ symmetry with respect to the axis of interaction with benzene). Similar bonding considerations should apply to the dianionic ketimide model systems $\{(\mu\text{-}\eta^6,\eta^6\text{-}C_6H_6)[U(NCH_2)_3]_2\}^{2-}$ (Figure 8). On the basis of this bonding scheme, the corresponding monoanionic ketimide complexes $[\mu\text{-arene-}\mathbf{1}_2]^-$ would be $S = {}^3/_2$ systems, with only three U-centered electrons. The monoanions $[\mu\text{-arene-}\mathbf{1}_2]^-$ would also feature a pair of δ backbonds that characterize arene binding.

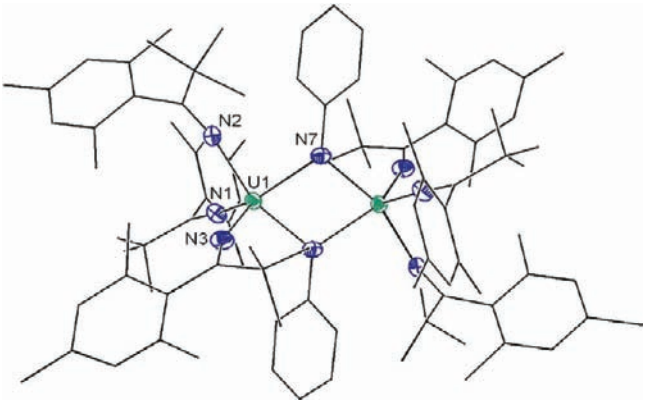

Figure 7. Structural drawing of complex **4** with thermal ellipsoids at the 35% probability level; H atoms have been omitted for clarity.

An intuitive way to assess the importance of δ back-bonding in early actinide chemistry is by its analogy to π back-bonding in transition-metal chemistry (Figure 9). The parallel between π back-bonding in transition-metal complexes and δ back-bonding in early actinide compounds is based on the fact that each bond involves half of the total lobes in a specific orbital (two out of four in the case of d orbitals and four out of eight in the case of f orbitals) when interacting with LUMOs of the ligand in question.

Bonding Considerations for Neutral μ-η^6,η^6-Arene-Bridged Diuranium Complexes. The benzene-bridged system $(\mu\text{-}\eta^6,\eta^6\text{-}C_6H_6)[U(NH_2)_2]_2$ has been adopted as a computational model with reference to the crystallographically determined structure of $(\mu\text{-}\eta^6,\eta^6\text{-toluene})[U(N[Ad]Ar)_2]_2$. Amsterdam Density Functional (ADF)[70−72] calculations were carried out, specifying a spin polarization equal to four (four unpaired electrons). Pictures of the key molecular orbitals (MOs) for $(\mu\text{-}\eta^6,\eta^6\text{-}C_6H_6)[U(NH_2)_2]_2$ are shown in Figure 10. A first noteworthy point is the excellent energy match between the LUMOs of uncomplexed benzene and the manifold of uranium-based orbitals (see Figure SX9 in the Supporting Information for details). Together with good overlap, this energy match leads to a strong stabilization of the four δ-bonding electrons found in MOs formed by U f orbitals and the LUMOs of benzene (Figure 10). The four unpaired electrons are located at ca. −2.5 eV, immediately below a dense manifold of virtual orbitals. There is a large energy difference of ca. 4 eV between the benzene HOMO and the uranium valence manifold such that electron donation from the benzene HOMO to uranium—an interaction of π symmetry with reference to the U−U axis—accounts for little of the bonding. Weak interactions involving the benzene HOMO can be discerned (PI and PI STAR in Figure SX9 in the Supporting Information).

The model $(\mu\text{-}\eta^6,\eta^6\text{-}C_6H_6)[U(NH_2)_2]_2$ reproduces well the observed structure of $(\mu\text{-}\eta^6,\eta^6\text{-toluene})[U(N[Ad]Ar)_2]_2$ (see the Supporting Information for details). Because covalent overlap of filled U orbitals with the benzene LUMOs

dx.doi.org/10.1021/ic202163m | Inorg. Chem. 2012, 51, 2902−2916

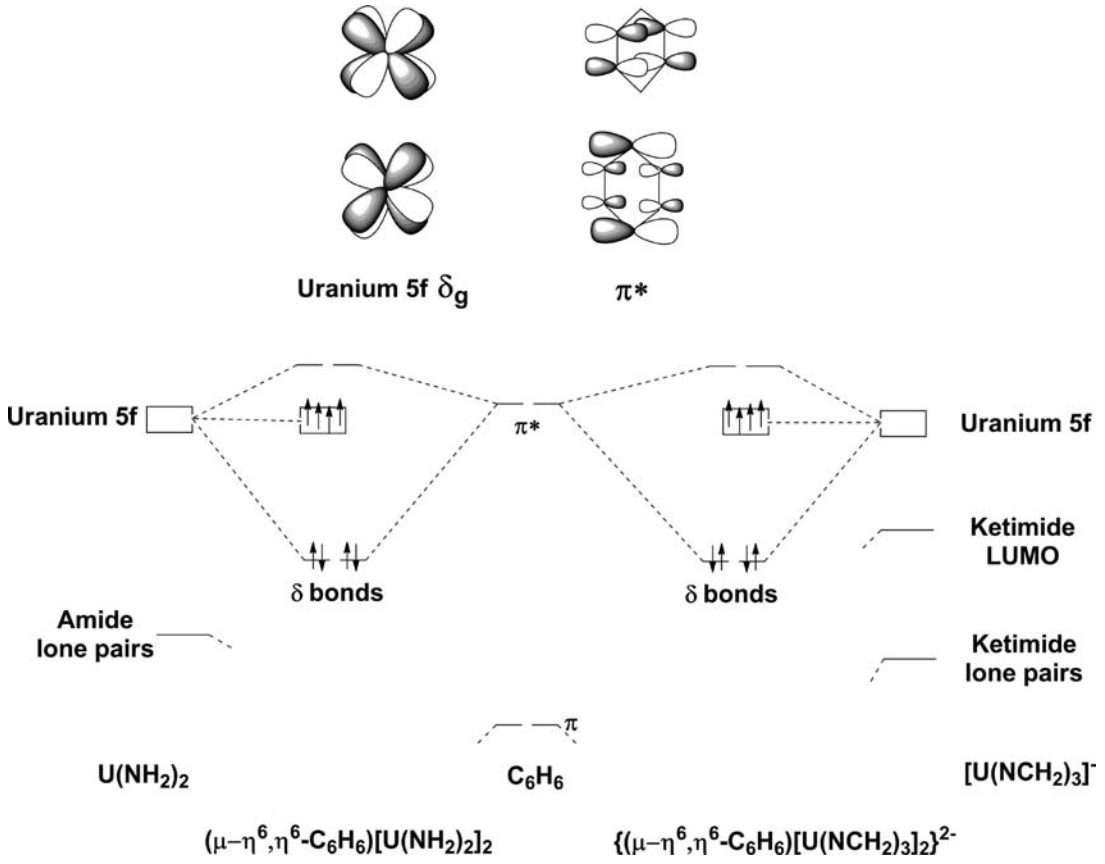

Figure 8. Schematic representation of frontier MOs for (μ-η^6,η^6-C_6H_6)-bridged diuranium complexes emphasizing the similarity between the neutral amide model systems (μ-η^6,η^6-C_6H_6)[$U(NH_2)_2$]$_2$ (left) and the dianionic ketimide model systems $\{(\mu\text{-}\eta^6,\eta^6\text{-}C_6H_6)[U(NCH_2)_3]_2\}^{2-}$ (right); orbital energies not drawn to scale.

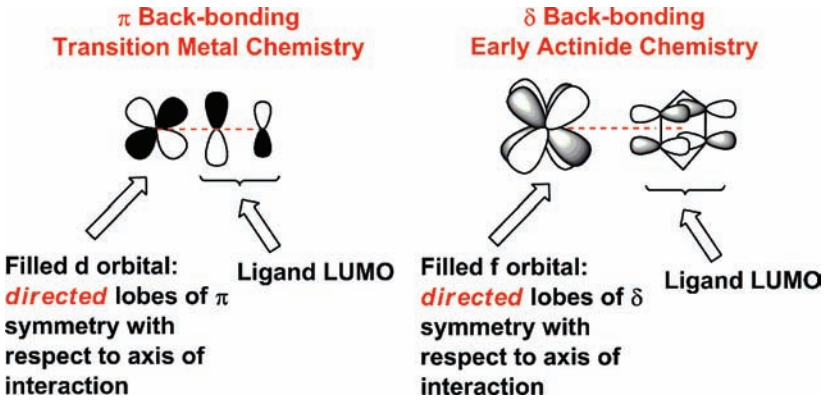

Figure 9. Comparison between π back-bonding in transition-metal chemistry and δ back-bonding in early actinide chemistry.

constitutes the principal interaction, it is natural that the C−C distances should be long relative to free benzene. The magnitude of the calculated elongation is ca. 0.07 Å, while the observed elongation is ca. 0.05 Å. Reproduced rather well are the short U−C distances of ca. 2.6 Å. Another interesting result from the DFT calculations is association of the spin density with the atoms present: essentially, all of the spin density is U-localized (Figure 8); very little spin density is associated with the C atoms of the bridging benzene. Thus, (μ-η^6,η^6-toluene)[U(N[Ad]Ar)$_2$]$_2$ cannot be construed as an ionically sandwiched benzene radical anion; although DFT calculations tend to overestimate the importance of covalency in organometallic complexes,[2,73,74] our results show that the mechanism of charge transfer from U to C is one of covalent overlap, i.e., δ back-bonding.

Bonding in Dianionic μ-η^6,η^6-Arene Diuranium Hexakisketimide Complexes. [Na(OH$_2$)$_3$]$_2$(μ-η^6,η^6-C_6H_6)[U(NCH$_2$)$_3$]$_2$ was chosen as a computational model for M$_2$(μ-η^6,η^6-arene)[U(NC^{t}BuMes)$_3$]$_2$. This model reproduces the key structural elements of the dianions [μ-arene-$\mathbf{1}_2$]$^{2-}$, including the ion-pairing interactions characterized by contacts between two ketimide N atoms per alkali-metal cation, and nominal five-coordination at each alkali metal (see the Supporting Information for details).

It should be mentioned that the ketimide ligand class, represented generically by N=C(R^1)(R^2), is expected to

dx.doi.org/10.1021/ic202163m | Inorg. Chem. 2012, 51, 2902−2916

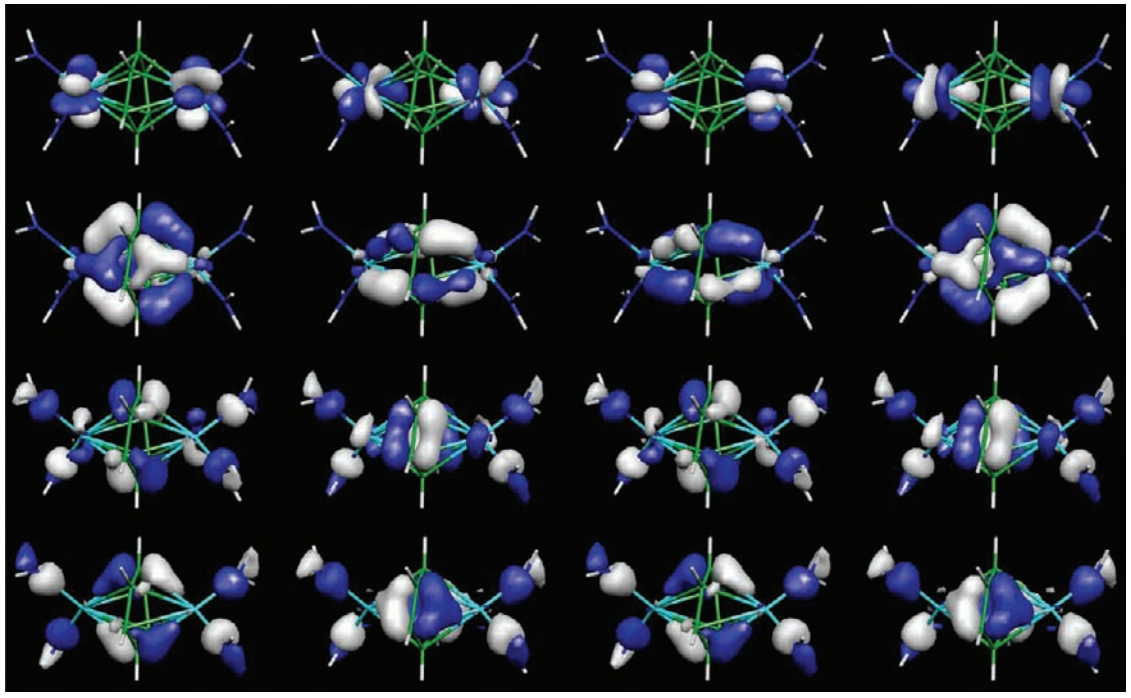

Figure 10. Selected orbitals for model system $(\mu\text{-}\eta^6,\eta^6\text{-}C_6H_6)[U(NH_2)_2]_2$. Top row from left to right: the F NONBONDING orbitals 32 B_3 α, 34 B_2 α, 31 B_1 α, and 36 A α. Second row: the DELTA orbitals 33 B_2 β, 35 A β, 35 A α, and 33 B_2 α. Third row: the PI STAR orbitals 29 B_1 β, 30 B_3 β, 29 B_1 α, and 30 B_3 α. Bottom row: the PI orbitals 28 B_1 β, 29 B_3 β, 28 B_1 α, and 29 B_3 α. Note that each depicted orbital corresponds to a single electron (spin-unrestricted formalism).

exhibit π-donor character in the trigonal plane defined by C and its N, R^1, and R^2 substituents; in the plane perpendicular to this, these ligands are expected to have π-acid character by virtue of the N═C π^* orbital. Thus, this ligand type is well suited to the stabilization of a negatively charged system. Accordingly, it was interesting to find that the unpaired spin density associated with $[Na(OH_2)_3]_2(\mu\text{-}\eta^6,\eta^6\text{-}C_6H_6)[U(NCH_2)_3]_2$ (S = 2) was not localized solely on the U centers but rather was delocalized onto the ketimide C atoms by the mechanism of π back-bonding (top row of MOs in Figure 11). These four MOs correspond to the four unpaired electrons in the previous systems, and because of the delocalization, their energies (Figure SX13) are depressed such that they separate out clearly below the dense manifold of low-lying virtual orbitals. The multipole-derived (MD) spin density[76] is essentially negligible on all atoms except for the U centers (ca. −1.1 each) and the ketimide ligand C atoms (ca. −0.5 each). For comparison, the MD spin density[76] per uranium in the neutral model system $(\mu\text{-}\eta^6,\eta^6\text{-}C_6H_6)[U(NH_2)_2]_2$ was −1.8. Thus, the ketimide ligands, while being strong π donors in one plane, also assist in the stabilization of negatively charged systems by virtue of their π-acid character.

In the energy-level diagram for $[Na(OH_2)_3]_2(\mu\text{-}\eta^6,\eta^6\text{-}C_6H_6)[U(NCH_2)_3]_2$ (Figure SX13 in the Supporting Information), four manifolds of orbitals are separated clearly from each other: metal-centered stabilized by π back-bonding to the ketimide ligands (four high-lying electrons, denoted as F-NONBONDING in Figure SX13 in the Supporting Information), covalent δ overlap between benzene LUMO and the two U centers (next highest-lying four electrons, denoted as DELTA), ketimide π-donor functions (12 electrons denoted as KETIMIDE LP), and the benzene HOMO that does not overlap covalently with the U centers (four electrons denoted as PI). Figure 11 displays these orbitals graphically, omitting those corresponding to ketimide π donation.

The bonding model proposed by us for dianions $[\mu\text{-arene-}\mathbf{1_2}]^{2-}$ considers them to be S = 2 systems, with the four unpaired electrons resident in uranium-based orbitals that are stabilized by π back-bonding to the peripheral ketimide ligands (Figure 11). Accordingly, we expect the corresponding monoanions $[\mu\text{-arene-}\mathbf{1_2}]^-$ to be $S = {}^3/_2$ systems, with only three such U-centered π back-bonding electrons. The monoanions $[\mu\text{-arene-}\mathbf{1_2}]^-$ would retain a full complement of four δ-bonding electrons for arene binding. Using the same computational methods as those discussed above, unfortunately, we have not been able to achieve convergence for a model monoanion, e.g., salt $[Na(OH_2)_3](\mu\text{-}\eta^6,\eta^6\text{-}C_6H_6)[U(N{=}CH_2)_3]_2$; therefore, detailed computational elucidation of the electronic structure of monoanions $[\mu\text{-arene-}\mathbf{1_2}]^-$ will be deferred to future work.

Isolobal Relationship with Vanadium Triple-Decker Systems. Electronic structure calculations on $(\mu\text{-}\eta^6,\eta^6\text{-}C_6H_6)[VCp]_2$ were carried out by Chesky and Hall in 1984.[75] They pointed out that this system's MOs are easily identified with those of the cylindrical $D_{\infty h}$ point group and may be labeled accordingly as σ, π, or δ; furthermore, they remarked on the strong stabilization of a doubly degenerate δ pair of CpV linear combinations (containing four electrons) by the benzene LUMOs, making δ back-bonding the primary interaction between benzene and the two CpV fragments. As for $(\mu\text{-}\eta^6,\eta^6\text{-toluene})[U(N[Ad]Ar)_2]_2$, the ground state for $(\mu\text{-}\eta^6,\eta^6\text{-}C_6H_6)[VCp]_2$ was suggested to have S = 2.[75]

In order to compare $(\mu\text{-}\eta^6,\eta^6\text{-}C_6H_6)[U(NH_2)_2]_2$ and $(\mu\text{-}\eta^6,\eta^6\text{-}C_6H_6)[VCp]_2$, we performed new calculations on $(\mu\text{-}\eta^6,\eta^6\text{-}C_6H_6)[VCp]_2$ using the same methods as those employed for $(\mu\text{-}\eta^6,\eta^6\text{-}C_6H_6)[U(NH_2)_2]_2$. The calculated C−C distances for the sandwiched benzene ring are ca. 1.45 Å, in

dx.doi.org/10.1021/ic202163m | Inorg. Chem. 2012, 51, 2902−2916

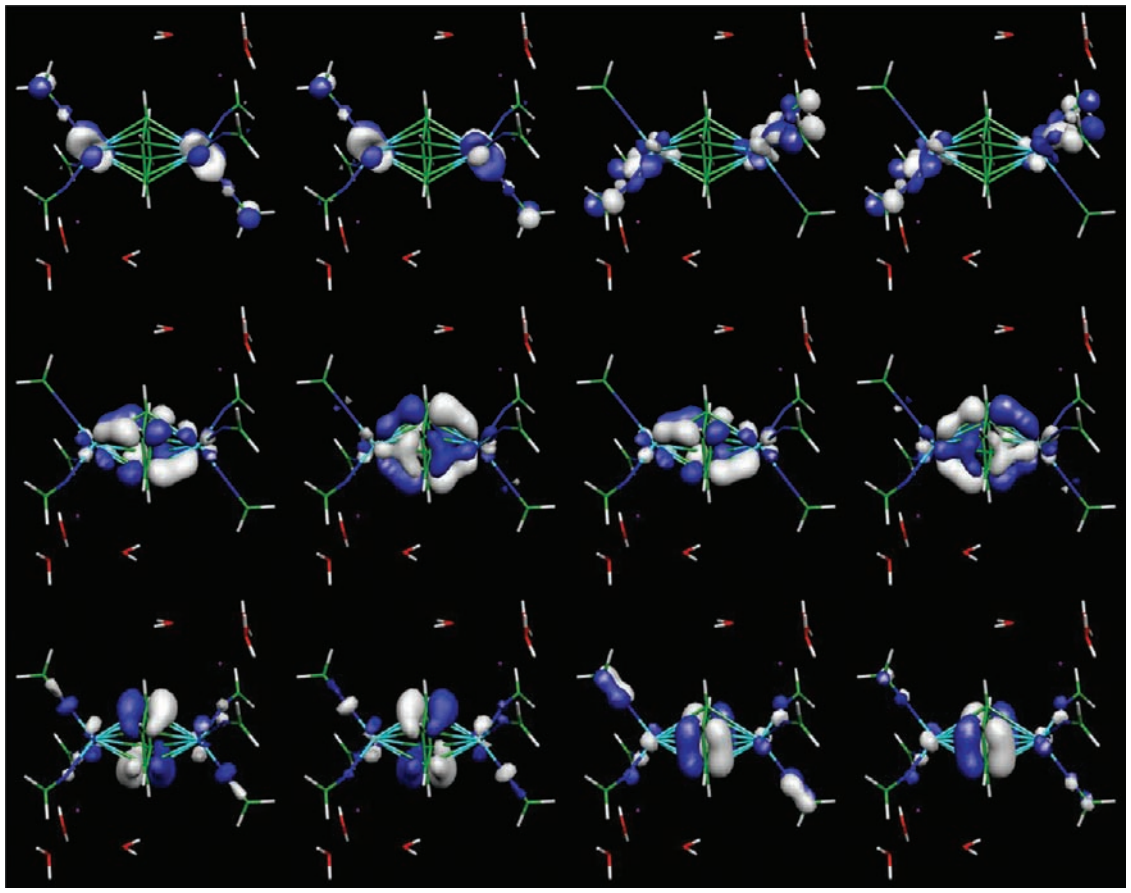

Figure 11. Selected MOs for $[Na(OH_2)_3]_2(\mu\text{-}\eta^6,\eta^6\text{-}C_6H_6)[U(NCH_2)_3]_2$ in order of decreasing energy from top left to bottom right. Top row: four electrons of spin α that have no spin β counterpart; note that these are not completely metal-localized but engage in back-bonding to the ketimide ligands. Middle row: four δ-bonding electrons in orbitals comprised of covalent uranium/benzene LUMO overlap. Bottom row: four electrons derived from the benzene HOMOs in orbitals that do not show U−C covalent overlap.

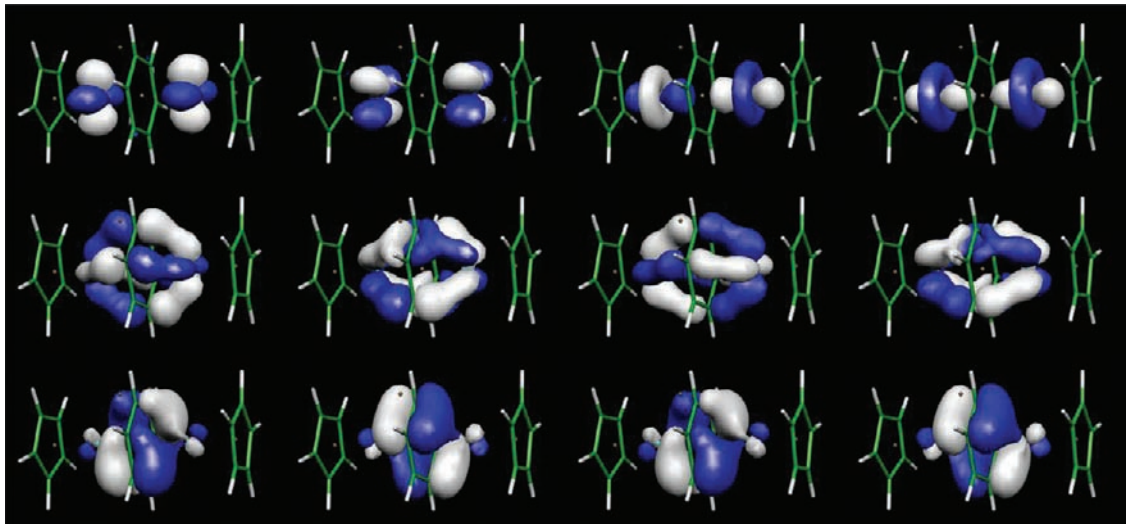

Figure 12. Selected MOs as calculated for $(\mu\text{-}\eta^6,\eta^6\text{-}C_6H_6)[VCp]_2$ in C_{2h} symmetry with the spin-unrestricted formalism and four spin-α electrons in excess (each pictured orbital represents a single electron). Top row from left to right: 14 B_g α, 27 A_g α, 26 B_u α, and 26 A_g α. The top row corresponds to the molecule's four unpaired electrons. Middle row: 14 A_u β, 25 B_u β, 14 A_u α, and 25 B_u α. The middle row corresponds to the two δ back-bonding orbitals constructed from the LUMOs of the bridging benzene and filled V d orbitals of appropriate symmetry. Bottom row: 24 A_g β, 12 B_g β, 24 A_g α, and 12 B_g α. The bottom row corresponds to the interaction of the benzene HOMOs with V-acceptor orbitals of π symmetry.

good agreement with those determined by X-ray crystallography (see the Supporting Information for details).[16] As found for $(\mu\text{-}\eta^6,\eta^6\text{-}C_6H_6)[U(NH_2)_2]_2$, the frontier MOs contain the four electrons involved in δ bonding and also the four electrons of spin α that have no spin β counterpart (Figure 12). In addition, the HOMO of free benzene, at lower than −6 eV, is a

dx.doi.org/10.1021/ic202163m | *Inorg. Chem.* 2012, 51, 2902−2916

poor match energetically for the metal-based orbitals. Overall, the four unpaired electrons occupy σ_g, σ_u, and δ_g orbitals, strong covalent δ_u bonding (4e) is observed, and the four electrons derived from the π_g benzene HOMO enjoy little stabilization by vanadium. In short, two d^4 CpV fragments interact with a μ-η^6,η^6-C_6H_6 ligand in a fashion isolobal with two f^4 $(H_2N)_2U$ fragments. Both systems can be construed as enjoying a maximum (4e) of δ back-bonding to the bridging ring and have an $S = 2$ ground state, with little spin density on the bridging ring.

CONCLUSIONS

The ketimide ligand NC^{t}BuMes has facilitated the isolation of several new arene-bridged diuranium complexes, all featuring three ketimide ligands per U center and inclusion of alkali-metal counterions. Reduction of the iodide trisketimide complex **1**-I(DME) with 4 equiv of KC_8 in DME in the presence of stoichiometric amounts of arene was found to be a general route to a series of dipotassium salts, K_2(μ-η^6,η^6-arene)[U(NC^{t}BuMes)$_3$]$_2$ (arene = naphthalene, biphenyl, *trans*-stilbene, and *p*-terphenyl). Crystallographic characterization for arene = biphenyl and *trans*-stilbene revealed in both cases a characteristic elongation of ca. 0.05 Å of arene C−C distances in the bridging ring, in accordance with findings from our DFT calculations. The magnitude of the C−C elongation upon complexation is similar to that reported for the transition-metal analogue (μ-η^6,η^6-benzene)[VCp]$_2$, with which the uranium complexes were found to be isolobal.

This study also revealed that the μ-η^6,η^6-arene diuranium hexakisketimide complexes are available in a higher oxidation state. Specifically, salts of monoanions [(μ-η^6,η^6-arene)[U(NC^{t}BuMes)$_3$]$_2$]$^-$ were synthesized for arenes such as naphthalene, biphenyl, *trans*-stilbene, *p*-terphenyl, toluene, and benzene. In cases where a 1:1 correspondence exists, i.e., with the exception of the benzene and toluene complexes, the chemical interconversion of the mono- and dianionic forms was successful.

Reactivity patterns established for the μ-η^6,η^6-arene diuranium hexakisketimide complexes show that they are susceptible to oxidation by a variety of reagents, leading most frequently to uranium(IV) and occasionally to uranium(V) products. Reactions with diphenyldisulfide and azobenzene provided new phenylthiolate- and phenylimido-bridged systems, respectively, while reactions with cyclooctatetraene provided a new entry into U(COT) half-sandwich chemistry. In all cases studied thus far, redox reactions of μ-η^6,η^6-arene diuranium hexakisketimide complexes give rise to arene expulsion, consistent with the notion that the arene is held in place by a pair of electron-rich U centers engaged in electron donation to the arene LUMO. The observed reactivity suggests that the dianionic μ-η^6,η^6-arene diuranium hexakisketimide complexes can be construed as uranium(II) synthons.

Overall, the μ-η^6,η^6-arene diuranium hexakisketimide motif represents, by virtue of variability in the choice of both the arene and state of charge, an example of a highly tunable reactive organometallic entity.

EXPERIMENTAL SECTION

General Considerations. Unless stated otherwise, all operations were performed in a Vacuum Atmospheres drybox under an atmosphere of purified nitrogen or using Schlenk techniques under an argon atmosphere. Anhydrous diethyl ether was purchased from Mallinckrodt; *n*-pentane, *n*-hexane, and tetrahydrofuran (THF) were purchased from EM Science. Diethyl ether, toluene, benzene, *n*-pentane, and *n*-hexane were dried and deoxygenated by the method of Grubbs et al.[77] THF and DME were distilled under nitrogen from purple sodium benzophenone ketyl. Distilled solvents were transferred under vacuum into glass vessels before being pumped into a Vacuum Atmospheres drybox. C_6D_6 and toluene-d_8 were purchased from Cambridge Isotopes and were degassed and dried over 4 Å sieves. Naphthalene-d_8, biphenyl-d_{10}, and *p*-terphenyl-d_{14} were purchased from Cambridge Isotopes. Naphthalene, α-naphthalene-d_1,[78] naphthalene-d_8, biphenyl, biphenyl-d_{10}, *o*-biphenyl-d_1,[78] *p*-biphenyl-d_1,[78] *p*-terphenyl, and *p*-terphenyl-d_{14} were dissolved in THF, and their solutions passed through alumina, concentrated, and placed in a −35 °C refrigerator. The crystals obtained were dried extensively under vacuum (at least 3 h) before use. 1,3,5,7-Cyclooctatetraene was passed through alumina and stored in a refrigerator at −35 °C. Sieves (4 Å), alumina, and Celite were dried in vacuo overnight at a temperature just above 200 °C. Compounds KC_8,[79] **1**-I(DME),[33] M_2[μ-naph-**1**$_2$],[33] M[(COT)U(NC[^{t}Bu]Mes)$_3$] (M = Na or K),[33] and (μ-η^8,η^8-COT)U$_2$(NC[^{t}Bu]Mes)$_6$[33] were prepared according to literature methods. Other chemicals were used as received. ^{1}H and ^{2}H NMR spectra were recorded on Varian XL-300 or Varian INOVA-501 spectrometers at room temperature unless otherwise specified. Chemical shifts are reported with respect to an internal or external solvent, 7.16 ppm (C_6D_6). UV−vis spectra were recorded on a HP spectrophotometer from 200 to 1100 nm using matched 1 cm quartz cells; all spectra were obtained using a solvent reference blank. Numerical modeling of all data was done using the program *Origin 6.0*. CHN analyses were performed by H. Kolbe Mikroanalytisches Laboratorium (Mülheim an der Ruhr, Germany).

*General Synthesis of Salts K$_2$[μ-arene-**1**$_2$] with That of K$_2$[μ-biph-**1**$_2$] Given as a Representative Example.* Compound **1**-I(DME) (0.532 g, 0.50 mmol, 2 equiv) and biphenyl (0.039 g, 0.25 mmol, 1 equiv) were dissolved in DME (15 mL), and the solution was frozen by placing the vessel containing it into the glovebox cold well. Separately, KC_8 (0.271 g, 2.00 mmol, 8 equiv) was slurried in DME (10 mL), and the slurry was also frozen. Both mixtures were removed from the cold well and allowed to thaw. The thawing KC_8 slurry was added dropwise to the thawing biphenyl/**1**-I(DME) solution. After complete addition, the reaction mixture was stirred at ca. 25 °C for 25 min and then filtered through Celite. After solvent removal from the filtrate, the dark-brown solid was extracted with pentane (ca. 100 mL), the extract was filtered through Celite, and the filtrate was taken to dryness. The crude residue thus obtained was mixed with diethyl ether (10 mL), whereupon the mixture was transferred to a vial and stored in a −35 °C refrigerator for several days. Decantation of the mother liquor and drying under reduced pressure gave a first crop of solid K$_2$[μ-biph-**1**$_2$] amounting to 0.223 g (0.23 mmol, 46% yield). A second crop (ca. 0.050 g) was subsequently obtained, giving a total yield of 56% (0.28 mmol). ^{1}H NMR (500 MHz, toluene-d_8, 20 °C): δ 34.04 (s, $\nu_{1/2}$ = 22 Hz, 1H, bound *p*-biphenyl), 8.30 (s, 12H, *m*-Ar). 3.74 (s, 18H, *p*-Me), 3.03 (s, 36H, *o*-Me), −3.09 (s, 54H, ^{t}Bu), −5.78 (s, $\nu_{1/2}$ = 6 Hz, 1H, pendant *p*-biphenyl), −21.40 (s, $\nu_{1/2}$ = 17 Hz, 2H, pendant *o*-biphenyl), −47.13 (s, $\nu_{1/2}$ = 48 Hz, 2H, pendant *m*-biphenyl), −73.53 (s, very broad, 2H, bound *m*-biphenyl), −126.56 (s, $\nu_{1/2}$ = 64 Hz, 2H, bound *o*-biphenyl). UV−vis (Et$_2$O, 22 °C): λ_{max}, nm ($\varepsilon \times 10^{-2}$, M^{-1} cm^{-1}) = 212 (2555.7 ± 110.1), 244 (808.6 ± 38.5), 282 (476.4 ± 24.8), 395 (152.2 ± 8.6). Anal. Calcd for $C_{96}H_{130}N_6K_2U_2$: C, 59.98; H, 6.82; N, 4.37. Found: C, 60.06; H, 6.48; N, 4.11.

*K$_2$[μ-biph-**1**$_2$-d_{10}].* This was synthesized as described for K$_2$[μ-biph-**1**$_2$], substituting biphenyl-d_{10} for biphenyl. ^{2}H NMR (46 MHz, Et$_2$O, 22 °C): δ 33.98 (s, 1D), −5.72 (s, 1D), −21.45 (s, 2D), −46.85 (s, 2D), −79.75 (s, 2D), −126.24 (s, 2D).

*K$_2$[μ-biph-**1**$_2$-2-d_1].* This was synthesized as described for K$_2$[μ-biph-**1**$_2$], substituting biphenyl-2-d_1 for biphenyl. ^{2}H NMR (46 MHz, Et$_2$O, 22 °C): δ −21.05 (s, 1D), −125.43 (s, 1D).

*K$_2$[μ-biph-**1**$_2$-4-d_1].* This was synthesized as described for K$_2$[μ-biph-**1**$_2$], substituting biphenyl-4-d_1 for biphenyl. ^{2}H NMR (46 MHz, Et$_2$O, 22 °C): δ 34.31 (s, 1D), −5.53 (s, 1D).

dx.doi.org/10.1021/ic202163m | *Inorg. Chem.* 2012, 51, 2902−2916

Na_2[μ-biph-1_2]. Sodium (0.030 g, 1.30 mmol, 3.5 equiv) was added to a THF solution (6 mL) of biphenyl (0.172 g, 1.12 mmol, 3 equiv) in a vial protected from light (with electrical tape), and the resulting mixture was stirred at room temperature for 1 h, after which time the vial was placed in the glovebox cold well. Separately, a solution of **1**-I(DME) (0.400 g, 0.38 mmol) in THF (10 mL) was frozen. The mixtures were then removed from the cold well and allowed to thaw. The thawing sodium/biphenyl mixture was added dropwise to the solution of **1**-I(DME), including the piece of sodium. The reaction mixture was allowed to reach room temperature and was stirred for 2 h, after which time the solution was decanted from the sodium piece and filtered. After removal from the filtrate of all volatile materials under reduced pressure, the crude solid residue thus obtained was extracted with pentane. The extract was filtered through Celite, and pentane was evaporated from the filtrate. Pentane extraction/filtration was repeated, leading to a new filtrate (5 mL), which was placed in a −35 °C refrigerator overnight. The mother liquor was then decanted from the solid obtained (biphenyl with traces of Na_2[μ-biph-$\mathbf{1}_2$]) and concentrated. The solid thus obtained was extracted with pentane (3 mL) followed by diethyl ether, but the two filtrates were not combined at this stage. Diethyl ether was removed from the filtered ether extract, and the solid obtained was extracted with pentane. At this point, the pentane extracts were combined, the solution was concentrated, and the concentrate was placed in a −35 °C refrigerator. Salt Na_2[μ-biph-$\mathbf{1}_2$] was obtained as a microcrystalline powder in 57% yield (0.204 g, 0.11 mmol) after 1 day. ^{1}H NMR (300 MHz, C_6D_6, 22 °C): δ 9.92 (s, 1H, bound *p*-biphenyl), 8.05 (s, 12H, *m*-Ar), 3.48 (s, 18H, *p*-Me), 2.50 (s, 36H, *o*-Me), −3.31 (s, 54H, ^{t}Bu), −1.23 (s, 1H, pendant *p*-biphenyl), −14.97 (s, 2H, pendant *o*-biphenyl), −55.88 (s, 2H, pendant *m*-biphenyl), −76.03 (s, 2H, bound *m*-biphenyl), −109.10 (s, 2H, bound *o*-biphenyl). Anal. Calcd for $C_{96}H_{130}N_6U_2Na_2$: C, 61.00; H, 6.93; N, 4.45. Found: C, 60.90; H, 7.56; N, 4.34.

K_2[μ-stilb-1_2]. The same procedure as that described above for K_2[μ-biph-$\mathbf{1}_2$], substituting *trans*-stilbene for biphenyl; the yield was 63% for the first crop of solid material, collected from *n*-pentane after 10 days. ^{1}H NMR (500 MHz, C_6D_6, 22 °C): δ 71.48 (br s, *trans*-stilbene), 8.76 (s, 12H, *m*-Ar), 8.58 (s, 18H, *p*-Me), 4.12 (s, 36H, *o*-Me), −3.04 (s, 54H, ^{t}Bu), −3.81 (br s, *trans*-stilbene), −24.25 (br s, *trans*-stilbene), −33.30 (br s, *trans*-stilbene), −35.04 (br s, *trans*-stilbene), −48.58 (br s, *trans*-stilbene), −144.18 (br s, *trans*-stilbene), −153.84 (br s, *trans*-stilbene). UV−vis (Et_2O, 22 °C): λ_{max}, nm (ε × 10^{-2}, M^{-1} cm^{-1}) = 210 (2554.0 ± 305.6), 280 (648.4 ± 99.1), 290 (350.7 ± 14.8), 353 (153.0 ± 8.5), 610 (93.0 ± 10.0). Anal. Calcd for $C_{98}H_{132}N_6K_2U_2$: C, 60.41; H, 6.83; N, 4.31. Found: C, 60.21; H, 6.56; N, 4.30.

K_2[μ-terph-1_2]. The same procedure as that described above for K_2[μ-biph-$\mathbf{1}_2$], substituting *p*-terphenyl for biphenyl; the yield was 67% for the first crop of solid material, collected from *n*-pentane after 7 days. ^{1}H NMR (500 MHz, toluene-d_8, 22 °C): δ 21.74 (s, $\nu_{1/2}$ = 93 MHz, 1H, *p*-bound *p*-terphenyl), 8.22 (s, 12H, *m*-Ar), 7.56 (m, 2H, pendant *p*-terphenyl), 5.43 (m, 1H, *p*-pendant *p*-terphenyl), 3.76 (s, 18H, *p*-Me), 3.38 (m, 2H, unbound *p*-terphenyl), 2.88 (s, 36H, *o*-Me), 2.23 (m, 2H, pendant *p*-terphenyl), −2.36 (s, 54H, ^{t}Bu), −17.71 (s, $\nu_{1/2}$ = 20 MHz, 2H, pendant *p*-terphenyl), −49.79 (s, $\nu_{1/2}$ = 61 MHz, 2H, bound *p*-terphenyl), −123.53 (s, $\nu_{1/2}$ = 76 MHz, 2H, bound *p*-terphenyl). UV−vis (Et_2O, 22 °C): λ_{max}, nm (ε × 10^{-2}, M^{-1} cm^{-1}) = 214 (2646.8 ± 136.0), 246 (1032.0 ± 142.1), 273 (820.9 ± 76.7), 494 (103.9 ± 10.0). Anal. Calcd for $C_{102}H_{134}N_6K_2U_2$: C, 61.30; H, 6.76; N, 4.21. Found: C, 61.51; H, 6.48; N, 4.12.

K_2[μ-terph-1_2-d_{14}]. The same procedure as that described above for K_2[μ-biph-$\mathbf{1}_2$], substituting *p*-terphenyl-d_{14} for biphenyl. ^{2}H NMR (76 MHz, Et_2O, 22 °C): δ 22.28 (s, 1D), 8.16 (s, 2D), 6.00 (s, 1D), 3.84 (s, 2D), 2.89 (s, 2D), −17.84 (s, 2D), −49.76 (s, 2D), −123.71 (s, 2D).

General Synthesis of Salts K[μ-arene-1_2] with That of K[μ-naph-1_2] Given as a Representative Example. Compound **1**-I(DME) (0.492 g, 0.46 mmol, 1 equiv) and naphthalene (0.030 g, 0.23 mmol, 0.5 equiv) were dissolved in DME (15 mL), and the solution was frozen in the glovebox cold well. Separately, KC_8 (0.125 g, 0.92 mmol, 2 equiv) was slurried in DME (12 mL), and the slurry was also frozen. Both frozen mixtures were removed from the cold well and permitted to thaw. The thawing KC_8 slurry was added dropwise to the thawing solution of **1**-I(DME) and naphthalene, with vigorous magnetic stirring. After complete addition, the reaction mixture was stirred for 20 min and then filtered through Celite. Solvent removal from the filtrate provided a dark-brown solid, which was extracted with pentane (ca. 100 mL). The pentane extract was filtered through Celite. Solvent removal from the filtrate provided a solid that was next slurried in a 2:1 mixture of pentane and diethyl ether (total of 10 mL), transferred to a vial, and stored in a −35 °C refrigerator for 1 day. The mother liquor was decanted, and the microcrystalline solid thus obtained was dried under reduced pressure, giving a first crop of K[μ-naph-$\mathbf{1}_2$] (0.251 g, 0.13 mmol, 56% yield). ^{1}H NMR (300 MHz, C_6D_6, 22 °C): δ 20.22 (s, 6H, *m*′-Ar), 9.34 (s, 6H, *p*′-Me), 8.93 (s, 8H, *m*-Ar), 4.49 (s, 12H, *o*′- or *p*-Me), 3.65 (s, 12H, *o*′- or *p*-Me), 1.29 (s, 36H, ^{t}Bu), −0.14 (s, 18H, ^{t}Bu′), −1.19 (s, 2H, pendant α-naphthalene), −2.19 (s, 24H, *o*-Me), −37.96 (s, 2H, pendant β-naphthalene), −121.17 (s, 2H, bound α-naphthalene), −124.53 (s, 2H, bound β-naphthalene). UV−vis (toluene, 22 °C): λ_{max}, nm (ε × 10^{-2}, M^{-1} cm^{-1}) = 282 (376.7 ± 28.4), 388 (134.9 ± 12.1), 632 (47.5 ± 7.4). Anal. Calcd for $C_{94}H_{128}N_6KU_2$: C, 60.79; H, 6.95; N, 4.53. Found: C, 60.70; H, 6.86; N, 4.70.

K[μ-naph-1_2-d_8]. The same preparation as that for K[μ-naph-$\mathbf{1}_2$] substituting naphthalene-d_8 for naphthalene. ^{2}H NMR (46 MHz, Et_2O, 22 °C): δ −0.46 (s, 1D), −38.97 (s, 1D), −117.73 (s, 1D), −126.53 (s, 1D).

K[μ-naph-1_2-d_1]. The same preparation as that for K[μ-naph-$\mathbf{1}_2$] substituting α-naphthalene-d_1 for naphthalene. ^{2}H NMR (46 MHz, Et_2O, 22 °C): δ −0.42 (s, 1D), −117.49 (s, 1D).

K[μ-biph-1_2]. The same preparation as that for K[μ-naph-$\mathbf{1}_2$] substituting biphenyl for naphthalene; yield 42% for the first crop (collected after 3 days, from pentane/Et_2O). ^{1}H NMR (300 MHz, C_6D_6, 22 °C): δ 16.86 (s, 6H, pendant *m*-biphenyl and *m*′-Ar), 8.96 (s, 8H, *m*-Ar), 7.95 (s, 6H, *p*′-Me), 4.50 (s, 12H, *o*′- or *p*-Me), 3.91 (s, 12H, *o*′- or *p*-Me), 1.02 (s, 36H, ^{t}Bu), 0.02 (s, 18H, ^{t}Bu′), −2.17 (s, 24H, *o*-Me), −9.19 (s, 2H, pendant *o*-biphenyl), −14.18 (s, 1H, pendant *p*-biphenyl), −83.57 (s, 1H, bound *p*-biphenyl), −140.72 (s, 2H, bound *m*-biphenyl), −163.87 (s, 2H, bound *o*-biphenyl). UV−vis (toluene, 22 °C): λ_{max}, nm (ε × 10^{-2}, M^{-1} cm^{-1}) = 285 (354.8 ± 23.3), 431 (188.4 ± 17.9), 647 (45.2 ± 4.1). Anal. Calcd for $C_{96}H_{130}N_6KU_2$: C, 61.22; H, 6.96; N, 4.46. Found: C, 60.74; H, 6.48; N, 3.94.

K[μ-biph-1_2-d_{10}]. The same procedure as that for K[μ-naph-$\mathbf{1}_2$] substituting biphenyl-d_{10} for naphthalene. ^{2}H NMR (46 MHz, Et_2O, 22 °C): δ 17.02 (s, 2D), −9.14 (s, 2D), −13.87 (s, 1D), −83.62 (s, 1D), −141.20 (s, 2D), −164.92 (s, 2D).

K[μ-biph-1_2-2-d_1]. The same procedure as that for K[μ-naph-$\mathbf{1}_2$] substituting biphenyl-2-d_1 for naphthalene. ^{2}H NMR (46 MHz, Et_2O, 22 °C): δ −9.20 (s, 1D), −164.46 (s, 1D).

K[μ-biph-1_2-4-d_1]. The same procedure as that for K[μ-naph-$\mathbf{1}_2$] substituting biphenyl-4-d_1 for naphthalene. ^{2}H NMR (46 MHz, Et_2O, 22 °C): δ −14.02 (s, 1D), −82.99 (s, 1D).

K[μ-stilb-1_2]. The same procedure as that for K[μ-naph-$\mathbf{1}_2$] substituting *trans*-stilbene for naphthalene; isolated yield 83% for the first crop of crystalline solid (1 day, pentane). ^{1}H NMR (500 MHz, C_6D_6, 22 °C): δ 16.64 (s, 4H, *m*′-Ar), 16.08 (br s, *trans*-stilbene), 9.47 (s, 6H, *p*′-Me), 8.01 (s, 8H, *m*-Ar), 4.81 (s, 12H, *o*′- or *p*-Me), 4.10 (s, 12H, *o*′- or *p*-Me), 0.63 (s, 36H, ^{t}Bu), −0.44 (s, 18H, ^{t}Bu′), −2.11 (s, 24H, *o*-Me), −46.02 (br s, *trans*-stilbene), −71.89 (br s, *trans*-stilbene). UV−vis (Et_2O, 22 °C): λ_{max}, nm (ε × 10^{-2}, M^{-1} cm^{-1}) = 215 (2118.9 ± 103.3), 282 (532.9 ± 56.2), 382 (150.3 ± 5.4), 568 (97.3 ± 4.7). Anal. Calcd for $C_{98}H_{132}N_6KU_2$: C, 61.65; H, 6.97; N, 4.40. Found: C, 61.68; H, 6.81; N, 4.40.

K[μ-terph-1_2]. The same procedure as that for K[μ-naph-$\mathbf{1}_2$] substituting *p*-terphenyl for naphthalene; isolated yield 69% for the first crop of crystalline solid (1 day, pentane). ^{1}H NMR (500 MHz, toluene-d_8, 22 °C): δ 18.11 (s, 2H, pendant *p*-terphenyl), 11.32 (m, 2H, pendant *p*-terphenyl), 8.88 (s, 8H, *m*-Ar), 7.97 (s, 6H, *p*′-Me), 7.51 (m, 1H, *p*-pendant *p*-terphenyl), 6.17 (m, 2H, pendant *p*-terphenyl), 4.39 (s, 12H, *o*′- or *p*-Me), 3.95 (s, 12H, *o*′- or *p*-Me),

dx.doi.org/10.1021/ic202163m | *Inorg. Chem.* 2012, 51, 2902−2916

0.89 (s, 36H, ^{t}Bu), −0.12 (s, 18H, ^{t}Bu′), −1.75 (s, 24H, *o*-Me), −7.35 (s, 2H, pendant *p*-terphenyl), −81.17 (s, $\nu_{1/2}$ = 106 Hz, 1H, *p*-bound *p*-terphenyl), −142.44 (s, $\nu_{1/2}$ = 78 Hz, 2H, *m*- or *o*-bound *p*-terphenyl), −163.31 (s, $\nu_{1/2}$ = 156 Hz, 2H, *m*- or -o-bound *p*-terphenyl). UV−vis (toluene, 22 °C): λ_{max}, nm ($\varepsilon \times 10^{-2}$, M^{-1} cm^{-1}) = 285 (552.9 ± 27.2), 447 (199.1 ± 7.8), 517 (174.2 ± 7.8). Anal. Calcd for $C_{102}H_{134}N_6KU_2$: C, 62.52; H, 6.89; N, 4.29. Found: C, 62.57; H, 6.90; N, 4.06.

*K[μ-terph-**1**$_2$-d_{14}].* The same procedure as that for K[μ-naph-**1**$_2$] substituting *p*-terphenyl-d_{14} for naphthalene. ^{2}H NMR (76 MHz, toluene, 22 °C): δ 18.87 (s, 2D), 12.17 (s, 2D), 8.45 (s, 1D), 6.83 (s, 2D), −5.84 (s, 2D), −88.13 (s, 1D), −145.85 (s, 2D), −162.39 (s, 2D).

*Synthesis of [K$_2$I][μ-tol-**1**$_2$].* A solution of **1**-I(DME) (2.075 g, 1.95 mmol) in 60 mL of toluene and a slurry of KC_8 (0.527 g, 3.90 mmol, 2 equiv) in 100 mL of toluene were frozen in the glovebox cold well, then taken out, and allowed to thaw. To the thawing solution of **1**-I(DME) was added dropwise the thawing KC_8 slurry. The reaction mixture was stirred for 2 h at ca. 25 °C and then filtered through Celite. The solvent was removed from the filtrate, the resulting solid was extracted with diethyl ether (100 mL), and the extract was filtered. The filtrate was concentrated to 10 mL and then placed in a −35 °C refrigerator for several days. Salt [K$_2$I][μ-tol-**1**$_2$] was thereby obtained as a dark-orange-brown microcrystalline solid (0.852 g, 0.43 mmol, 44% yield). ^{1}H NMR (300 MHz, C_6D_6, 22 °C): δ 34.70 (s, 3H, toluene-C*H*$_3$), 6.98 (s, 12H, *m*-Ar), 2.53 (s, 18H, *p*-Me), 1.63 (s, 54H, ^{t}Bu), 1.50 (s, 36H, *o*-Me), −38.01 (s, 2H, *o*- or *m*-toluene), −43.05 (s, 1H, *p*-toluene), −44.63 (s, 2H, *o*- or *m*-toluene). UV−vis (Et_2O, 22 °C): λ_{max}, nm ($\varepsilon \times 10^{-2}$, M^{-1} cm^{-1}) = 214 (2099.2 ± 255.7), 267 (593.3 ± 108.6), 432 (120.5 ± 10.5), 541 (80.7 ± 8.1). Anal. Calcd for $C_{84}H_{120}N_6U_2K_2I$: C, 55.03; H, 6.45; N, 4.23. Found: C, 54.45; H, 5.85; N, 3.92.

[K$_2$I][μ-tol-**1**$_2$-d_8] was prepared as described for [K$_2$I][μ-tol-**1**$_2$-d_8], substituting toluene-d_8 for toluene. ^{2}H NMR (76 MHz, pentane, 22 °C): δ 34.42 (s, 3D, C*D*$_3$-toluene), −37.76 (s, 2D, *o*- or *m*-toluene), −42.73 (s, 1D, *p*-toluene), −44.43 (s, 2D, *o*- or *m*-toluene).

*Synthesis of [K$_2$I][μ-benz-**1**$_2$].* A solution of **1**-I(DME) (0.090 g, 0.08 mmol) in 8 mL of benzene and a slurry of KC_8 (0.023 g, 0.17 mmol, 2 equiv) in 4 mL of benzene were frozen by placing the vessels containing them into the glovebox cold well. Subsequently, said vessels were taken out of the cold well and allowed to thaw. To the thawing solution of **1**-I(DME) was added dropwise the thawing KC_8 slurry. The reaction mixture was stirred for 20 min, after which it was filtered through Celite and the volatiles were removed from the filtrate under reduced pressure. After extraction of the residue with pentane, the extract (20 mL) was concentrated to 3 mL and cooled to −35 °C. The crystals of [K$_2$I][μ-benz-**1**$_2$] (0.018 g, 0.009 mmol, 11% yield) so obtained were used to prepare an NMR sample, leading to the following data: ^{1}H NMR (300 MHz, C_6D_6, 22 °C): δ 6.97 (s, 2H, *m*-Ar), 2.57 (s, 3H, *p*-Me), 1.87 (s, 9H, ^{t}Bu), 1.36 (s, 6H, *o*-Me), −44.91 (s, 1H, C_6H_6).

*Synthesis of [K(DME)][μ-tol-**1**$_2$].* Complex **1**-I(DME) (0.163 g, 0.15 mmol) and toluene (3 drops, ca. 0.030 g, 0.33 mmol, 2.2 equiv) were dissolved in DME (5 mL), and the solution was frozen by placing the vessel containing it into the glovebox cold well. Separately, KC_8 (0.062 g, 0.46 mmol, 3 equiv) was slurried in DME (3 mL) and the slurry was also frozen. Both mixtures were then taken out of the cold well and allowed to thaw. The thawing KC_8 slurry was then added dropwise to the thawing solution of complex **1**-I(DME). After complete addition, the reaction mixture was stirred for 20 min and then filtered through Celite. After solvent removal from the filtrate, the resulting dark-brown solid was extracted with pentane (ca. 15 mL), the pentane extract was filtered through Celite, and the pentane was removed from the filtrate by assisted evaporation. The resulting crude solid was extracted with pentane (10 mL), and the extract was filtered through Celite, concentrated to 3 mL, and stored in a −35 °C refrigerator for several days. A first crop of [K(DME)][μ-tol-**1**$_2$] crystals (0.061 g, 0.03 mmol, 41% yield) was obtained by decanting the mother liquor and drying under reduced pressure. ^{1}H NMR (500 MHz, toluene-d_8, 22 °C): δ 64.48 (s, 3H, C*H*$_3$-toluene), 8.61 (s, 12H, *m*-Ar), 4.15 (s, 18H, *p*-Me), 3.36 (s, 4H, C*H*$_2$-DME), 3.15 (s, 6H, C*H*$_3$-DME), 1.22 (s, 36H, *o*-Me), −1.20 (s, 54H, ^{t}Bu), −109.52 (s, 2H, *o*- or *m*-toluene), −113.84 (s, 2H, *o*- or *m*-toluene), −126.52 (s, 1H, *p*-toluene). UV−vis (Et_2O, 22 °C): λ_{max}, nm ($\varepsilon \times 10^{-2}$, M^{-1} cm^{-1}) = 214 (2099.2 ± 255.7), 267 (593.3 ± 108.6), 432 (120.5 ± 10.5), 541 (80.7 ± 8.1). Anal. Calcd for $C_{95}H_{138}N_6U_2O_2K$: C, 59.70; H, 7.28; N, 4.40. Found: C, 60.10; H, 7.17; N, 4.59.

*[K(DME)][μ-tol-**1**$_2$-d_8].* The same procedure as that described for [K(DME)][μ-tol-**1**$_2$], substituting toluene-d_8 for toluene. ^{2}H NMR (76 MHz, pentane, 22 °C): δ 63.42 (s, 3D, C*D*$_3$-toluene), −107.23 (s, 2D, *o*- or *m*-toluene), −114.43 (s, 2D, *o*- or *m*-toluene), −127.73 (s, 1D, *p*-toluene).

*[K(DME)][μ-benz-**1**$_2$].* The same procedure as that described for [K(DME)][μ-tol-**1**$_2$], substituting benzene for toluene. ^{1}H NMR (300 MHz, C_6D_6, 22 °C): δ 8.43 (s, 12H, *m*-Ar), 3.98 (s, 18H, *p*-Me), 3.07 (s, 4H, C*H*$_2$-DME), 2.85 (s, 6H, C*H*$_3$-DME), 1.47 (s, 36H, *o*-Me), −0.78 (s, 54H, ^{t}Bu), −112.83 (s, 1H, C_6H_6).

*Oxidation of K$_2$[μ-arene-**1**$_2$] to K[μ-arene-**1**$_2$] Using Fc[OTf].* *Note:* Only the oxidation of K$_2$[μ-stilb-**1**$_2$] to K[μ-stilb-**1**$_2$] is described in detail, with the reactions for the other three K$_2$[μ-arene-**1**$_2$] being similar. Solutions of K$_2$[μ-stilb-**1**$_2$] (0.253 g, 0.13 mmol) and Fc[OTf] (0.044 g, 0.13 mmol, 1 equiv) in diethyl ether were frozen. The thawing K$_2$[μ-stilb-**1**$_2$] solution was added dropwise to the thawing Fc[OTf] solution, and the reaction mixture was allowed to reach room temperature and stirred for 1 h. After that time, the mixture was filtered through Celite, and the volatiles were removed. The solid obtained was extracted with pentane, and the solution obtained was filtered through Celite, concentrated, and placed in a −35 °C refrigerator. After 8 days, K[μ-stilb-**1**$_2$] was obtained as a microcrystalline solid (0.200 g, 0.10 mmol) in 81% yield.

*Oxidation of K$_2$[μ-arene-**1**$_2$] to K[μ-arene-**1**$_2$] Using P$_4$.* *Note:* Only the oxidation of K$_2$[μ-stilb-**1**$_2$] to K[μ-stilb-**1**$_2$] is described in detail, with the reactions for the other three K$_2$[μ-arene-**1**$_2$] being similar. Solutions of K$_2$[μ-stilb-**1**$_2$] (0.109 g, 0.06 mmol) and P$_4$ (0.009 g, 0.07 mmol, 1.3 equiv) in diethyl ether were frozen. The thawing K$_2$[μ-stilb-**1**$_2$] solution was added dropwise to the thawing P$_4$ slurry; the reaction mixture was allowed to reach room temperature and stirred for 0.5 h. After that time, the mixture was filtered through Celite and the volatiles were removed. The solid obtained was extracted with pentane, and the solution obtained was filtered through Celite, concentrated, and placed in a −35 °C refrigerator. After 5 days, K[μ-stilb-**1**$_2$] was obtained as a microcrystalline solid (0.074 g, 0.10 mmol) in 69% yield.

*Reduction of K[μ-arene-**1**$_2$]to K$_2$[μ-arene-**1**$_2$] Using K/Anthracene.* *Note:* Only the reduction of K[μ-stilb-**1**$_2$] to K$_2$[μ-stilb-**1**$_2$] is described in detail, with the reactions for the other three K[μ-arene-**1**$_2$] being similar. Potassium (0.100 g, 2.6 mmol, 5.2 equiv) was added to a THF solution (3 mL) of anthracene (0.010 g, 0.05 mmol, 1 equiv) in a vial protected from light (with electrical tape), and the resulting mixture was stirred at room temperature for 1 h, after which time the vial was placed in a cold well. Separately, a solution of K[μ-stilb-**1**$_2$] (0.091 g, 0.05 mmol) in THF (2 mL) was frozen. The thawing K/anthracene mixture was added dropwise to the K[μ-stilb-**1**$_2$] solution, with the excess of potassium being left behind. The new mixture was allowed to reach room temperature and stirred for 1 h, after which time the solution was transferred to a filter flask. After removal of the volatiles under reduced pressure, the solid obtained was extracted in pentane, the extract filtered through Celite, and the pentane removed. A new extraction in pentane and filtration through Celite led to a new filtrate (5 mL), which was concentrated and placed in a refrigerator overnight. Compound K$_2$[μ-stilb-**1**$_2$] was obtained as a microcrystalline powder in 78% yield (0.073 g, 0.04 mmol) after several days.

*Synthesis of (η^8-C_8H_8)U(NC[^{t}Bu]Mes)$_3$ (**2**).* Solutions of K[**2**] (0.063 g, 0.06 mmol) and $TiCl_4(THF)_2$ (0.022 g, 0.06 mmol, 1 equiv) in diethyl ether (3 mL each) were frozen. To the thawing $TiCl_4(THF)_2$ solution was added dropwise the K[**2**] solution. The reaction mixture was stirred for 3 h at room temperature and then filtered through Celite. The solvent from the filtrate was removed and the solid extracted with pentane (5 mL) and then with diethyl ether. The solution was concentrated and then placed in a refrigerator for several

dx.doi.org/10.1021/ic202163m | *Inorg. Chem.* 2012, 51, 2902−2916

days. **2** was obtained as an orange-brown microcrystalline solid (0.035 g, 58% yield, 0.03 mmol). ^{1}H NMR (500 MHz, C_6D_6, 22 °C): δ 7.35 (s, 6H, *m*-Ar), 3.13 (s, 27H, ^{t}Bu), 2.70 (s, 9H, *p*-Me), 1.53 (s, 18H, *o*-Me), −14.84 (s, 8H, COT). Anal. Calcd for $C_{50}H_{68}N_3U$: C, 63.28; H, 7.22; N, 4.43. Found: C, 62.96; H, 7.22; N, 4.31.

*Reaction of Na$_2$[μ-naph-**1**$_2$] with PhSSPh.* *Note:* All of the reactions with PhSSPh were performed in a similar manner, with the results being different as discussed in the text. For K[μ-arene-**1**$_2$] compounds, 1.5 equiv of PhSSPh was used instead of 2 equiv. Solutions of Na$_2$[μ-naph-**1**$_2$] (0.232 g, 0.12 mmol) and PhSSPh (0.054 g, 0.25 mmol, 2 equiv) in diethyl ether (6 mL each) were frozen. To the thawing Na$_2$[μ-naph-**1**$_2$] solution was added dropwise the PhSSPh solution, and the reaction mixture was stirred for 1 h at room temperature. After that time, the solvent was removed and the solid extracted with pentane (10 mL). The solution was concentrated and then placed in a refrigerator for several days. Na[**3**] was obtained as a dark-brown microcrystalline solid (0.225 g, 0.10 mmol, 83% yield). ^{1}H NMR (500 MHz, C_6D_6, 60 °C): δ 8.80 (s, 2H, *o*- or *m*-PhS), 8.62 (s, 2H, *o*- or *m*-PhS), 7.80 (s, 4H, *m*-Ar), 6.65 (s, 1H, *p*-PhS), 3.97 (s, 6H, *p*-Me), 0.34 (s, 18H, ^{t}Bu), −1.51 (s, 12H, *o*-Me). Anal. Calcd for $C_{102}H_{135}N_6U_2NaS_3$: C, 60.06; H, 6.62; N, 4.12. Found: C, 60.65; H, 6.80; N, 4.01. Similarly, K[**3**] was obtained from K$_2$[μ-arene-**1**$_2$]. Anal. Calcd for $C_{102}H_{135}N_6U_2KS_3$: C, 59.65; H, 6.25; N, 4.09. Found: C, 59.24; H, 6.25; N, 3.91.

*Reaction of [K$_2$I][μ-tol-**1**$_2$] with PhNNPh.* Solutions of [K$_2$I][μ-tol-**1**$_2$] (0.300 g, 0.15 mmol) and PhNNPh (0.055 g, 0.30 mmol, 2 equiv) in diethyl ether (6 mL each) were frozen. To the thawing [K$_2$I][μ-tol-**1**$_2$] solution was added dropwise the PhNNPh solution, and the reaction mixture was stirred for 1 h at room temperature. After that time, the solvent was removed and the solid extracted with pentane (10 mL). The solution was concentrated and then placed in a refrigerator for several days. **4** was obtained as a dark-brown microcrystalline solid (0.178 g, 0.09 mmol, 63% yield). ^{1}H NMR (500 MHz, C_6D_6, 60 °C): δ 8.34 (m, 2H, *o*- or *m*-PhN), 6.80 (s, 6H, *m*-Ar), 2.52 (s, 9H, *p*-Me), 2.27 (s, 12H, *o*-Me), 0.64 (s, 27H, ^{t}Bu), 0.57 (m, 1H, *p*-PhN), −5.22 (m, 2H, *o*- or *m*-PhN). Anal. Calcd for $C_{96}H_{130}N_8U_2$: C, 61.62; H, 6.95; N, 5.99. Found: C, 61.92; H, 7.36; N, 6.31.

*Reaction of [K$_2$I][μ-tol-**1**$_2$] with PhNNPh-d_{10}.* The experimental procedure is similar to the one given for **4**, with PhNNPh-d_{10} being used instead of PhNNPh. ^{2}H NMR (76 MHz, Et$_2$O, 22 °C): δ 8.20 (s, 2D), 0.15 (s, 1D), −5.52 (s, 2D).

X-ray Crystal Structures: General Considerations. The X-ray data collections were carried out on a Siemens Platform three-circle goniometer with a CCD detector using Mo Kα radiation (λ = 0.710 73 Å). The data were processed utilizing the program *SAINT* supplied by Siemens Industrial Automation, Inc. The structures were solved by direct methods (Sheldrick, G. M. *SHELXTL*, version 5.03; Siemens Industrial Automation, Inc.: Madison, WI, 1995) in conjunction with standard difference Fourier techniques.[80]

■ ASSOCIATED CONTENT

Ⓢ Supporting Information

X-ray crystallographic data in CIF format, details of X-ray crystallography, and DFT calculations. This material is available free of charge via the Internet at http://pubs.acs.org.

■ AUTHOR INFORMATION

Corresponding Author

*E-mail: pld@chem.ucla.edu (P.L.D.), ccummins@mit.edu (C.C.C.).

Notes

The authors declare no competing financial interest.

■ ACKNOWLEDGMENTS

For support of this work, the authors are grateful to the National Science Foundation (Grant CHE-9988806) and the National Science Board (Alan T. Waterman Award to C.C.C., 1998). Permission to include material from P.L.D.'s Ph.D. thesis, for which MIT has the copyright, has been received, and it is given in the Supporting Information.

■ REFERENCES

(1) Bochkarev, M. N. *Chem. Rev.* **2002**, *102*, 2089.
(2) Kozimor, S. A.; Yang, P.; Batista, E. R.; Boland, K. S.; Burns, C. J.; Clark, D. L.; Conradson, S. D.; Martin, R. L.; Wilkerson, M. P.; Wolfsberg, L. E. *J. Am. Chem. Soc.* **2009**, *131*, 12125.
(3) Cesari, M.; Pedretti, U.; Zazzetta, Z.; Lugli, G.; Marconi, W. *Inorg. Chim. Acta* **1971**, *5*, 439.
(4) Plíva, J.; Johns, J. W. C.; Goodman, L. *J. Mol. Spectrosc.* **1990**, *140*, 214.
(5) Kukolich, S. G. *J. Am. Chem. Soc.* **1995**, *117*, 5512.
(6) Cotton, F. A.; Schwotzer, W. *Organometallics* **1987**, *6*, 1275.
(7) Baudry, D.; Bulot, E.; Charpin, P.; Ephritikhine, M.; Lance, M.; Nierlich, M.; Vigner, J. *J. Organomet. Chem.* **1989**, *371*, 155.
(8) Baudry, D.; Bulot, E.; Ephritikhine, M. *J. Chem. Soc., Chem. Commun.* **1988**, 1369.
(9) Van der Sluys, W. G.; Burns, C. J.; Huffman, J. C.; Sattelberger, A. P. *J. Am. Chem. Soc.* **1988**, *110*, 5924.
(10) Li, J.; Bursten, B. E. *J. Am. Chem. Soc.* **1999**, *121*, 10243.
(11) Hong, G.; Dolg, M.; Li, L. *Int. J. Quantum Chem.* **2000**, *80*, 201.
(12) Diaconescu, P. L.; Arnold, P. L.; Baker, T. A.; Mindiola, D. J.; Cummins, C. C. *J. Am. Chem. Soc.* **2000**, *122*, 6108.
(13) Korobkov, I.; Gambarotta, S.; Yap, G. P. A. *Angew. Chem., Int. Ed.* **2003**, *42*, 814.
(14) Warner, B. P.; Scott, B. L.; Burns, C. J. *Angew. Chem., Int. Ed.* **1998**, *37*, 959.
(15) Zi, G.; Jia, L.; Werkema, E. L.; Walter, M. D.; Gottfriedsen, J. P.; Andersen, R. A. *Organometallics* **2005**, *24*, 4251.
(16) Duff, A. W.; Jonas, K.; Goddard, R.; Kraus, H. J.; Krueger, C. *J. Am. Chem. Soc.* **1983**, *105*, 5479.
(17) Nikiforov, G. B.; Crewdson, P.; Gambarotta, S.; Korobkov, I.; Budzelaar, P. H. M. *Organometallics* **2006**, *26*, 48.
(18) Tsai, Y.-C.; Wang, P.-Y.; Chen, S.-A.; Chen, J.-M. *J. Am. Chem. Soc.* **2007**, *129*, 8066.
(19) Monillas, W. H.; Yap, G. P. A.; Theopold, K. H. *Angew. Chem., Int. Ed.* **2007**, *46*, 6692.
(20) Tsai, Y.-C.; Wang, P.-Y.; Lin, K.-M.; Chen, S.-A.; Chen, J.-M. *Chem. Commun.* **2008**, 205.
(21) Ni, C.; Ellis, B. D.; Fettinger, J. C.; Long, G. J.; Power, P. P. *Chem. Commun.* **2008**, 1014.
(22) Cassani, M. C.; Duncalf, D. J.; Lappert, M. F. *J. Am. Chem. Soc.* **1998**, *120*, 12958.
(23) Gun'ko, Y. K.; Hitchcock, P. B.; Lappert, M. F. *Organometallics* **2000**, *19*, 2832.
(24) Thiele, K.-H.; Bambirra, S.; Schumann, H.; Hemling, H. *J. Organomet. Chem.* **1996**, *517*, 161.
(25) Arliguie, T.; Lance, M.; Nierlich, M.; Vigner, J.; Ephritikhine, M. *J. Chem. Soc., Chem. Commun.* **1994**, 847.
(26) Arliguie, T.; Lance, M.; Nierlich, M.; Ephritikhine, M. *J. Chem. Soc., Dalton Trans.* **1997**, *14*, 2501.
(27) Evans, W. J.; Kozimor, S. A.; Ziller, J. W.; Kaltsoyannis, N. *J. Am. Chem. Soc.* **2004**, *126*, 14533.
(28) Evans, W. J.; Traina, C. A.; Ziller, J. W. *J. Am. Chem. Soc.* **2009**, *131*, 17473.
(29) Evans, W. J.; Kozimor, S. A. *Coord. Chem. Rev.* **2006**, *250*, 911.
(30) Mills, D. P.; Moro, F.; McMaster, J.; van Slageren, J.; Lewis, W.; Blake, A. J.; Liddle, S. T. *Nat. Chem.* **2011**, *3*, 454.
(31) Monreal, M. J.; Khan, S. I.; Kiplinger, J. L.; Diaconescu, P. L. *Chem. Commun.* **2011**, *47*, 9119.
(32) Patel, D.; Moro, F.; McMaster, J.; Lewis, W.; Blake, A. J.; Liddle, S. T. *Angew. Chem., Int. Ed.* **2011**, *50*, 10388.
(33) Diaconescu, P. L.; Cummins, C. C. *J. Am. Chem. Soc.* **2002**, *124*, 7660.

(34) Fryzuk, M. D.; Jafarpour, L.; Kerton, F. M.; Love, J. B.; Rettig, S. J. *Angew. Chem., Int. Ed.* **2000**, *39*, 767.
(35) Evans, W. J.; Allen, N. T.; Ziller, J. W. *J. Am. Chem. Soc.* **2000**, *122*, 11749.
(36) Kirillov, E. N.; Trifonov, A. A.; Nefedov, S. E.; Eremenko, I. L.; Edelmann, F. T.; Bochkarev, M. N. *Z. Naturforsch.* **1999**, *54b*, 1379.
(37) Bochkarev, M. N.; Fedushkin, I. L.; Larichev, R. B. *Russ. Chem. Bull. Int. Ed.* **1996**, *45*, 2443.
(38) Fedushkin, I. L.; Bochkarev, M. N.; Schumann, H.; Esser, L.; Kociok- Kohn, G. *J. Organomet. Chem.* **1995**, *489*, 145.
(39) Basalgina, T. A.; Kalinina, G. S.; Bochkarev, M. N. *Organomet. Chem. USSR* **1989**, *2*, 606.
(40) Bochkarev, M. N.; Trifonov, A. A.; Cherkasov, V. L.; Razuvaev, G. A. *Organomet. Chem. USSR* **1988**, *1*, 216.
(41) Bochkarev, M. N.; Fagin, A. A.; Fedushkin, I. L.; Trifonov, A. A.; Kirillov, E. N.; Eremenko, I. L.; Nefedov, S. E. *Mater. Sci. Forum* **1999**, *315*−*317*, 144.
(42) Bochkarev, M. N.; Fedushkin, I. L.; Fagin, A. A.; Schumann, H.; Demtschuk, J. J. *J. Chem. Soc., Chem. Commun.* **1997**, 1783.
(43) Fedushkin, I. L.; Nevodchikov, V. K.; Cherkasov, V. K.; Bochkarev, M. N.; Schumann, H.; Girgsdies, F.; Gorlitz, F. H.; Kociok-Köhn, G.; Pickardt, J. *J. Organomet. Chem.* **1996**, *511*, 157.
(44) Arakawa, T.; Shimada, S.; Adachi, G.-Y.; Shiokawa, J. *Inorg. Chim. Acta* **1988**, *145*, 327.
(45) Fedorova, E. A.; Glushkova, N. V.; Bochkarev, M. N.; Schumann, H.; Hemling, H. *Russ. Chem. Bull. Int. Ed.* **1996**, *45*, 1996.
(46) Bochkarev, M. N.; Trifonov, A. A.; Cherkasov, V. K.; Razuvaev, G. A. *J. Gen. Chem. USSR* **1988**, *58*, 637.
(47) Bochkarev, M. N. *Proc. Indian Natl. Sci. Acad.* **1989**, *55A*, 170.
(48) Bochkarev, M. N.; Trifonov, A. A.; Fedorova, E. A.; Emelyanova, N. S.; Basalgina, T. A.; Kalinina, G. S.; Razuvaev, G. A. *J. Organomet. Chem.* **1989**, *372*, 217.
(49) Huang, W.; Khan, S. I.; Diaconescu, P. L. *J. Am. Chem. Soc.* **2011**, *133*, 10410.
(50) Bush, B. F.; Lynch, V. M.; Lagowski, J. J. *Organometallics* **1987**, *6*, 1267.
(51) Elschenbroich, C.; Heck, J. *J. Am. Chem. Soc.* **1979**, *101*, 6773.
(52) Hargreaves, A.; Rizvi, S. H. *Acta Crystallogr., Sect. A* **1962**, *15*, 365.
(53) Trotter, J. *Acta Crystallogr., Sect. A* **1961**, *14*, 1135.
(54) Charbonneau, G. P.; Delugeard, Y. *Acta Crystallogr., Sect. B* **1976**, *32*, 1420.
(55) Sasaki, Y.; Hamaguchi, H *Spectrochim. Acta A* **1994**, *50*, 1475.
(56) Weiss, E. *Angew. Chem., Int. Ed. Engl.* **1993**, *32*, 1501.
(57) Clark, D. L.; Gordon, J. C.; Huffman, J. C.; Vincent-Hollis, R. L.; Watkin, J. G.; Zwick, B. D. *Inorg. Chem.* **1994**, *33*, 5903.
(58) Meyer, N.; Roesky, P. W.; Bambirra, S.; Meetsma, A.; Hessen, B.; Saliu, K.; Takats, J. *Organometallics* **2008**, *27*, 1501.
(59) Pan, C.-L.; Chen, W.; Song, J. *Organometallics* **2011**, *30*, 2252.
(60) Duval, P. B.; Burns, C. J.; Buschmann, W. E.; Clark, D. L.; Morris, D. E.; Scott, B. L. *Inorg. Chem.* **2001**, *40*, 5491.
(61) Fox, A. R.; Arnold, P. L.; Cummins, C. C. *J. Am. Chem. Soc.* **2010**, *132*, 3250.
(62) Hayton, T. W. *Dalton Trans.* **2010**, *39*, 1145.
(63) Berthet, J.-C.; Lance, M.; Nierlich, M.; Vigner, J.; Ephritikhine, M. *J. Organomet. Chem.* **1991**, *420*, C9.
(64) Meerholz, K.; Heinze, J. *J. Am. Chem. Soc.* **1989**, *111*, 2325.
(65) Martin, T. P. *Angew. Chem., Int. Ed. Engl.* **1986**, *25*, 197.
(66) Baudry, D.; Bulot, E.; Ephritikhine, M.; Nierlich, M.; Lance, M.; Vigner, J. *J. Organomet. Chem.* **1990**, *388*, 279.
(67) Berthet, J.-C.; Ephritikhine, M. *J. Chem. Soc., Chem. Commun.* **1993**, 1566.
(68) Boisson, C.; Berthet, J.-C.; Lance, M.; Vigner, J.; Nierlich, M.; Ephritikhine, M. *J. Chem. Soc., Dalton Trans.* **1996**, 947.
(69) Evans, A. G.; Evans, J. C.; Emes, P. J.; James, C. L.; Pomery, P. J. *J. Chem. Soc. B: Phys. Org.* **1971**, 1484.
(70) te Velde, G.; Bickelhaupt, F. M.; Baerends, E. J.; Fonseca Guerra, C.; van Gisbergen, S. J. A.; Snijders, J. G.; Ziegler, T. *J. Comput. Chem.* **2001**, *22*, 931.
(71) Fonseca Guerra, C.; Snijders, J. G.; te Velde, G.; Baerends, E. J. *Theor. Chem. Acc.* **1998**, *99*, 391.
(72) *ADF, SCM*; Theoretical Chemistry, Vrije Universiteit; Amsterdam, The Netherlands, http://www.scm.com.
(73) Szilagyi, R. K.; Metz, M.; Solomon, E. I. *J. Phys. Chem. A* **2002**, *106*, 2994.
(74) Atanasov, M.; Daul, C.; Güdel, H. U.; Wesolowski, T. A.; Zbiri, M. *Inorg. Chem.* **2005**, *44*, 2954.
(75) Chesky, P. T.; Hall, M. B. *J. Am. Chem. Soc.* **1984**, *106*, 5186.
(76) Swart, M.; van Duijnen, P. T.; Snijders, J. G. *J. Comput. Chem.* **2001**, *22*, 79.
(77) Pangborn, A. B.; Giardello, M. A.; Grubbs, R. H.; Rosen, R. K.; Timmers, F. J. *Organometallics* **1996**, *15*, 1518.
(78) Miura, Y.; Oka, H.; Yamano, E.; Morita, M. *J. Org. Chem.* **1997**, *62*, 1188.
(79) Schwindt, M. A.; Lejon, T.; Hegedus, L. S. *Organometallics* **1990**, *9*, 2814.
(80) Sheldrick, G. *Acta Crystallogr., Sect. A* **2008**, *64*, 112.